

# VIRTUAL ELEMENT APPROXIMATION OF EIGENVALUE PROBLEMS

DANIELE BOFFI, FRANCESCA GARDINI, AND LUCIA GASTALDI

**ABSTRACT.** We discuss the approximation of eigenvalue problems associated with elliptic partial differential equations using the virtual element method. After recalling the abstract theory, we present a model problem, describing in detail the features of the scheme, and highlighting the effects of the stabilizing parameters. We conclude the discussion with a survey of several application examples.

## 1. INTRODUCTION

In this chapter we discuss the use of the Virtual Element Method (VEM) for the approximation of eigenvalue problems associated with partial differential equations. Eigenvalue problems are present in several applications and are the object of an appealing and vast research area. It is known that the analysis of numerical schemes for the approximation of eigenmodes is based on suitable a priori estimates and appropriate compactness assumptions (see, for instance [28, 4, 10]).

Moreover, a good knowledge of the spectral properties of a discretization scheme is essential for the stability analysis of transient problems. It is well known, for instance, that the solution of parabolic and hyperbolic linear evolution problems (heat/wave equation) can be presented as a Fourier series in terms of eigenfunctions and eigenvalues of the corresponding elliptic eigenproblem (Laplace eigenproblem). We refer the interested reader to [35] for more information and to [14, 15] for an example of how things can go wrong if the eigenvalue problem is not correctly approximated.

The virtual element method has been successfully used for the approximation of several eigenvalue problems. Starting from the pioneering works [31, 26], where the analysis of the Steklov and the Laplace eigenproblems was developed, other applications of VEM to eigenvalue problems include an acoustic vibration problem [8], plates models [32, 34], linear elasticity [30], and a transmission problem [33]. Moreover, nonconforming,  $p$ , and  $hp$  VEM have been considered in [25, 36] for the Laplace eigenvalue problem.

The above mentioned references make use of classical tools for the spectral analysis, such as the Babuška–Osborn theory [4] for compact operators or the Descloux–Nassif–Rappaz theory [23] for non-compact operators, typically adopted in connection with a shift procedure. In the case of the mixed formulation for the Laplace eigenproblem [29], the conditions introduced in [12, 11] are considered.

---

2020 *Mathematics Subject Classification.* 65N30, 65N25.

*Key words and phrases.* partial differential equations, eigenvalue problem, parameter dependent matrices, virtual element method, polygonal meshes.

An important feature of VEM, as compared to standard FEM, is that suitable stabilizing forms, depending on appropriate parameters, have to be introduced in order to guarantee consistency and stability of the approximation. Typical theoretical results state that, for given choices of the stabilization parameters, the discrete solution converges to the continuous one with optimal order asymptotically in  $h$  or  $p$ . In the case of eigenvalue problems, the presence of the stabilizing forms may introduce artificially additional eigenmodes and we have to make sure that they will not pollute the portion of the spectrum we are interested in. Some of the above mentioned references address this issue even if they are not conclusive in this respect. In [13] we presented a systematic study of the eigenvalue dependence on the parameters. If the discrete eigenvalue can be written in the form  $\mathbf{A}u = \lambda \mathbf{M}u$ , with  $\mathbf{A}$  and  $\mathbf{M}$  depending on  $\alpha$  and  $\beta$ , respectively, then the *quick and easy recipe* is to pick a sufficiently large  $\alpha$  and a small (possibly zero)  $\beta$ . Such discussion is summarized in Section 5.

After describing the general setting of a variationally posed eigenvalue problem in Section 2, we recall the basic theory for the VEM approximation of the Laplace eigenproblem in Section 3. The case of nonconforming,  $p$ , and  $hp$  VEM is treated in Section 4. As already mentioned, Section 5 deals with the choice of the stabilizing parameters. Finally, Section 6 presents a survey of applications of VEM to the discretization of eigenproblems of interest.

## 2. ABSTRACT SETTING

Let  $V$  and  $H$  be two Hilbert spaces such that  $V \subset H$  with dense and compact embedding, and  $a(\cdot, \cdot)$  and  $b(\cdot, \cdot)$  be two continuous and symmetric bilinear forms defined on  $V \times V$  and  $H \times H$ , respectively. We consider the following eigenvalue problem in variational form: find  $(\lambda, u) \in \mathbb{R} \times V$  with  $u \neq 0$  such that

$$(1) \quad a(u, v) = \lambda b(u, v) \quad \forall v \in V.$$

The source problem associated with problem (1) reads: given  $f \in H$ , find  $u \in V$  such that

$$(2) \quad a(u, v) = b(f, v) \quad \forall v \in V.$$

We assume that  $a(\cdot, \cdot)$  is coercive on  $V$ , that is there exists  $\alpha > 0$  such that

$$a(v, v) \geq \alpha \|v\|_V^2 \quad \forall v \in V.$$

Under these assumptions, there exists a unique solution  $u \in V$  of problem (2) satisfying the following stability estimate

$$(3) \quad \|u\|_V \leq C \|f\|_H.$$

We then consider the solution operator  $T : H \rightarrow V \subset H$  defined as follows:

$$Tf = u, \quad u \in V,$$

with  $u$  the unique solution of the source problem (2). Since problem (2) is well posed,  $T$  is a well defined, self-adjoint linear bounded operator. Thanks to the compact embedding of  $V$  in  $H$ , it turns out that  $T$  is also compact. The same conclusions apply to the situation when  $V$  is not compact in  $H$ , by assuming directly the compactness of the operator  $T$ . We observe that  $(\lambda, u)$  is an eigenpair of problem (1) if and only if  $(\frac{1}{\lambda}, u)$  is an eigenpair of  $T$ . Thanks to the spectral

theory of compact operators, we have that the eigenvalues of problem (1) are real and positive and form a divergent sequence

$$(4) \quad 0 < \lambda_1 \leq \lambda_2 \leq \dots \leq \lambda_i \leq \dots;$$

conventionally, we repeat them according to their multiplicities. The corresponding eigenfunctions  $u_i$  are chosen with the following properties

$$\|u_i\|_H = 1, \quad a(u_i, u_i) = \lambda_i,$$

and so that they form an orthonormal basis both in  $V$  and in  $H$ .

We introduce a Galerkin type discretization of problems (1) and (2). To this end, let  $V_h \subset V$  be a finite dimensional subspace of  $V$ , and  $a_h : V_h \times V_h \rightarrow \mathbb{R}$  and  $b_h : H \times H \rightarrow \mathbb{R}$  two discrete symmetric continuous bilinear forms. Then, the discrete eigenvalue problem and the discrete source problems are given by: find  $(\lambda_h, u_h) \in \mathbb{R} \times V_h$  with  $u_h \neq 0$  such that

$$(5) \quad a_h(u_h, v_h) = \lambda_h b_h(u_h, v_h) \quad \forall v_h \in V_h,$$

and, given  $f \in H$ , find  $u_h \in V_h$  such that

$$(6) \quad a_h(u_h, v_h) = b_h(f, v_h) \quad \forall v_h \in V_h.$$

In order to guarantee existence, uniqueness, and stability of the solution to the discrete source problem (6), we assume that the discrete bilinear form  $a_h$  is coercive.

Similarly to the continuous case, we introduce the discrete solution operator  $T_h : H \rightarrow V_h \subset H$  defined by

$$T_h f = u_h,$$

with  $u_h \in V_h$  the unique solution to the discrete source problem (6).  $T_h$  is a self-adjoint operator with finite range, hence it is compact and has  $N_h$  positive discrete eigenvalues

$$0 < \lambda_{h,1} \leq \lambda_{h,2} \leq \dots \leq \lambda_{h,N_h},$$

where  $N_h$  denotes the dimension of  $V_h$ . Moreover, the discrete eigenfunctions  $u_{h,i}$  span  $V_h$  and can be chosen as an orthogonal basis satisfying

$$\|u_{h,i}\|_H = 1, \quad a(u_{h,i}, u_{h,i}) = \lambda_{h,i} \quad \forall i = 1, \dots, N_h.$$

We recall some results of the spectral approximation theory for compact operators [28, 4, 10]. In the following we denote by  $\delta(E, F)$  the gap between the spaces  $E$  and  $F$ , that is

$$\delta(E, F) = \max(\hat{\delta}(E, F), \hat{\delta}(F, E)) \quad \text{with} \quad \hat{\delta}(E, F) = \sup_{\substack{u \in E \\ \|u\|_H=1}} \inf_{v \in F} \|u - v\|_H.$$

**Theorem 1.** *Let us assume that*

$$(7) \quad \|T - T_h\|_{\mathcal{L}(H,H)} \rightarrow 0 \quad \text{as } h \rightarrow 0.$$

*Let  $\lambda_i$  be an eigenvalue of problem (1) with multiplicity equal to  $m$ , namely  $\lambda_i = \lambda_{i+1} = \dots = \lambda_{i+m-1}$ . Then, for  $h$  small enough such that  $N_h \geq i + m - 1$ , exactly  $m$  discrete eigenvalues  $\lambda_{h,i} = \lambda_{h,i+1} = \dots = \lambda_{h,i+m-1}$  converge to  $\lambda_i$ .*

*Moreover, let  $\mathcal{E}_i$  be the eigenspace of dimension  $m$  associated with  $\lambda_i$  and  $\mathcal{E}_{h,i} = \bigoplus_{j=i}^{i+m-1} \text{span}(u_{h,j})$  be the direct sum of the eigenspaces associated with the discrete eigenvalues. Then*

$$(8) \quad \delta(\mathcal{E}_i, \mathcal{E}_{h,i}) \rightarrow 0 \quad \text{as } h \rightarrow 0,$$

*where  $\delta(E, F)$  denotes the gap between the spaces  $E$  and  $F$ .*

**Theorem 2.** *Using the same notation as in Theorem 1, then there exists a positive constant  $C$  independent of  $h$  such that*

$$(9) \quad \delta(\mathcal{E}_i, \mathcal{E}_{h,i}) \leq C \|(T - T_h)|_{\mathcal{E}_i}\|_{\mathcal{L}(H,H)}.$$

Let  $\phi_1, \dots, \phi_m$  be a basis of the eigenspace  $\mathcal{E}_i$  corresponding to the eigenvalue  $\lambda_i$ . Then, for  $j = i, \dots, i + m - 1$

$$(10) \quad |\lambda_j - \lambda_{j,h}| \leq C \left( \sum_{l,k=1}^m |((T - T_h)\phi_k, \phi_l)_H| + \|(T - T_h)|_{\mathcal{E}_i}\|_{\mathcal{L}(H,H)} \right),$$

where  $(\cdot, \cdot)_H$  stands for the scalar product in  $H$ .

*Remark 1.* The solution operator could also be defined as  $T_V : V \rightarrow V$  such that for all  $f \in V$ ,  $T_V f$  is the solution to problem (2). If  $T_V$  is compact, then one can obtain results similar to those presented above with due modifications.

**2.1. Model Problem.** Let  $\Omega \subset \mathbb{R}^d$  ( $d = 2, 3$ ) be an open bounded Lipschitz domain. As a model problem, we consider the Laplace eigenvalue equation with homogeneous Dirichlet boundary conditions:

$$(11) \quad \begin{aligned} -\Delta u &= \lambda u && \text{in } \Omega \\ u &= 0 && \text{on } \partial\Omega. \end{aligned}$$

Setting

$$(12) \quad \begin{aligned} V &= H_0^1(\Omega) & H &= L^2(\Omega) \\ a(u, v) &= \int_{\Omega} \nabla u \cdot \nabla v \, dx & b(u, v) &= \int_{\Omega} uv \, dx \end{aligned}$$

the weak formulation of (11) fits the above abstract setting. Later on we will use the following additional regularity result [1, 27]: if  $f \in L^2(\Omega)$  there exists  $r \in (\frac{1}{2}, 1]$  such that  $u \in H^{1+r}(\Omega)$ , with

$$(13) \quad \|u\|_{1+r} \leq C \|f\|_0.$$

The regularity index  $r$  depends on the maximum interior wedge angle of  $\Omega$ . In particular, if the domain is convex  $r$  can be taken equal to 1.

Here and in what follows, we adopt the usual notation  $\|\cdot\|_{s,D}$  and  $|\cdot|_{s,D}$  for norm and seminorm in the Sobolev space  $H^s(D)$ . When  $D = \Omega$  we omit the subindex  $\Omega$ . Moreover, we set  $a^D(u, v) = \int_D \nabla u \cdot \nabla v \, dx$  and  $b^D(u, v) = \int_D uv \, dx$ .

### 3. VIRTUAL ELEMENT APPROXIMATION OF THE LAPLACE EIGENVALUE PROBLEM

In this section, we consider the Laplace eigenproblem and, after recalling the definition and the approximation properties of VEM, we present the discretization of the eigenvalue problem (1) and the relative convergence analysis. We treat in detail only the two dimensional case; for the three dimensional one, which can be analyzed with the same arguments, we refer to [26, 25].

**3.1. Virtual Element Method.** We denote by  $\mathcal{T}_h$  a family of polygonal decomposition of  $\Omega$ , by  $h_P$  the diameter of the element  $P \in \mathcal{T}_h$ , by  $h$  the maximum of such diameters, and by  $\mathcal{E}_h$  the set of the edges of the mesh. Moreover,  $\mathcal{E}_h^0$  and  $\mathcal{E}_h^\partial$  stand for the subset of internal and boundary edges, respectively.

We suppose that for all  $h$ , there exists a constant  $\rho$  such that each element  $P \in \mathcal{T}_h$  is star-shaped with respect to a disk with radius greater than  $\rho h_P$ , and for

every edge  $e \in \partial P$  it holds that  $h_e \geq \rho h_P$  (see [5]). We observe that the scaling assumption implies that the number of edges in the boundary of each element is uniformly bounded over the whole mesh family  $\mathcal{T}_h$ . However, there is no restriction on the interior angles of the polygons which can be convex, flat, or concave.

Let  $k \geq 1$  be a given integer, we denote by  $\mathbb{P}_k(P)$  the space of polynomials of degree at most equal to  $k$ . We introduce the *enhanced* virtual element space  $V_h$  of order  $k$  (see [2]). We consider the local space

$$(14) \quad V_h^k(P) = \left\{ v \in \tilde{V}_h^k(P) : \int_P (v - \Pi_k^\nabla v) p \, dx = 0 \quad \forall p \in (\mathbb{P}_k \setminus \mathbb{P}_{k-2})(P) \right\},$$

with the following definitions:

$$(15) \quad \begin{aligned} \tilde{V}_h^k(P) &= \{ v \in H^1(P) : v|_{\partial P} \in C^0(\partial P), v|_e \in \mathbb{P}_k(e) \quad \forall e \in \partial P, \Delta v \in \mathbb{P}_k(P) \} \\ \Pi_k^\nabla : \tilde{V}_h^k(P) &\rightarrow \mathbb{P}_k(P) \text{ is a projection operator defined by} \\ a^P(\Pi_k^\nabla v - v, p) &= 0 \quad \forall p \in \mathbb{P}_k(P) \\ \int_{\partial P} (\Pi_k^\nabla v - v) \, ds &= 0. \end{aligned}$$

In (14),  $(\mathbb{P}_k \setminus \mathbb{P}_{k-2})(P)$  stands for the space of polynomials in  $\mathbb{P}_k(P)$   $L^2$ -orthogonal to  $\mathbb{P}_{k-2}(P)$ .

As shown in [2], it is possible to compute  $\Pi_k^\nabla v_h$  for all  $v_h \in V_h^k(P)$  using the following degrees of freedom: the values  $v(V_i)$  at the vertices  $V_i$  of  $P$ , the scaled moments up to order  $k-2$  on each edge  $e \subset \partial P$ , and on the element  $P$ .

The global virtual element space is obtained by gluing together the local spaces, that is

$$V_h^k = \{ v \in H_0^1(\Omega) : v|_P \in V_h^k(P) \quad \forall P \in \mathcal{T}_h \}.$$

From now on, we denote by  $N_h$  the dimension of  $V_h^k$ .

We highlight that, differently from finite elements, we do not have at hand the explicit knowledge of the basis functions of  $V_h^k$ ; in this sense the basis functions are *virtual*. On the other hand, polynomials of degree at most  $k$  are in the VEM space; this will guarantee the optimal order of accuracy. Actually, the following approximation results hold true, see [17, 5, 20].

**Proposition 3.** *There exists a positive constant  $C$ , depending only on the polynomial degree  $k$  and the shape regularity  $\rho$ , such that for every  $s$  with  $1 \leq s \leq k+1$  and for every  $v \in H^s(\Omega)$  there exists  $v_\pi \in \mathbb{P}_k(P)$  such that*

$$(16) \quad \|v - v_\pi\|_{0,P} + h_P |v - v_\pi|_{1,P} \leq Ch_P^s |v|_{s,P}.$$

*Moreover, there exists a constant  $C$ , depending only on the polynomial degree  $k$  and the shape regularity  $\rho$ , such that for every  $s$  with  $1 \leq s \leq k+1$ , for every  $h$ , and for every  $v \in H^s(\Omega)$  there exists  $v_I \in V_h^k$  such that*

$$(17) \quad \|v - v_I\|_0 + h_P |v - v_I|_1 \leq Ch_P^s |v|_s.$$

Notice that  $v_\pi$  is defined element by element, and does not belong to the space  $H^1(\Omega)$ . We shall denote its broken  $H^1$ -seminorm by  $|v_\pi|_{1,h}$ .

**3.2. The VEM discretization of the Laplace eigenproblem.** In the VEM context, the discrete bilinear forms  $a_h(\cdot, \cdot)$  and  $b_h(\cdot, \cdot)$  are written as sum over the elements  $P \in \mathcal{T}_h$  of local contributions  $a_h^P(\cdot, \cdot)$  and  $b_h^P(\cdot, \cdot)$  for all  $P \in \mathcal{T}_h$ , that is

$$a_h(\cdot, \cdot) = \sum_{P \in \mathcal{T}_h} a_h^P(\cdot, \cdot), \quad b_h(\cdot, \cdot) = \sum_{P \in \mathcal{T}_h} b_h^P(\cdot, \cdot).$$

For the readers' convenience, we recall here the discrete source problem (6): given  $f \in L^2(\Omega)$ , find  $u_h \in V_h^k$  such that

$$(18) \quad a_h(u_h, v_h) = b_h(f, v_h) \quad \forall v_h \in V_h^k.$$

It is well known that solving this problem is equivalent to solve a linear system of equations  $\mathbf{A}u = \mathbf{f}$ , where  $\mathbf{A}$  is the  $N_h \times N_h$  matrix corresponding to the form  $a_h$  and  $\mathbf{f}$  is the vector with components  $b_h(f, \varphi_h)$  with  $\varphi_h$  the basis functions of  $V_h^k$ .

We now address the issue of the construction of the discrete bilinear forms along the lines of [5]. First of all, they are required to be similar to the continuous ones, namely

$$a_h^P(v_h, v_h) \approx a^P(v_h, v_h), \quad b_h^P(v_h, v_h) \approx b^P(v_h, v_h).$$

We underline that the continuous forms  $a(\cdot, \cdot)$  and  $b(\cdot, \cdot)$  in general are not computable on the basis functions, except for those which are polynomials. Hence we need to project the elements of  $V_h^k(P)$  onto  $\mathbb{P}_k(P)$ . This could be done locally as follows:

$$(19) \quad a_h^P(u_h, v_h) = a^P(\Pi_k^\nabla u_h, \Pi_k^\nabla v_h) \quad \forall u_h, v_h \in \mathcal{T}_h,$$

but it might happen that a non vanishing element  $u_h \in V_h^k(P)$  is such that  $\Pi_k^\nabla u_h = 0$ , and so the form  $a_h^P(u_h, v_h) = 0$  for all  $v_h \in V_h^k(P)$ . In this case the local contribution to the matrix  $\mathbf{A}_h$  results to be singular and the global matrix might lack control on some components of  $V_h^k$ . To avoid this eventuality, we add a stability term as follows:

$$(20) \quad a_h^P(u_h, v_h) = a^P(\Pi_k^\nabla u_h, \Pi_k^\nabla v_h) + S_a^P((I - \Pi_k^\nabla)u_h, (I - \Pi_k^\nabla)v_h),$$

where  $S_a^P(\cdot, \cdot)$  is a symmetric positive definite bilinear form defined on  $V_h^k(P) \times V_h^k(P)$  scaling like  $a^P(\cdot, \cdot)$ .

For proper choices of  $S_a^P$ , it turns out that  $a_h^P(\cdot, \cdot)$  fulfils the following local *stability* and *consistency* properties for all  $P \in \mathcal{T}_h$ .

**Stability::** there exists two positive constants  $a_*$  and  $a^*$  such that for all  $v_h \in V_h^k(P)$

$$(21) \quad a_* a^P(v_h, v_h) \leq a_h^P(v_h, v_h) \leq a^* a^P(v_h, v_h).$$

**Consistency::** for all  $v_h \in V_h^k(P)$  and for all  $p_k \in \mathbb{P}_k(P)$  it holds

$$(22) \quad a_h^P(v_h, p_k) = a^P(v_h, p_k).$$

In order to deal with the right hand side in (18), we define another projection operator  $\Pi_k^0$  from  $L^2(P)$  onto  $\mathbb{P}_k(P)$  as

$$b^P(\Pi_k^0 f, p_k) = b^P(f, p_k) \quad \forall p_k \in \mathbb{P}_k(P), \quad \forall P \in \mathcal{T}_h.$$

This projection operator is computable starting from the degrees of freedom as well. Thus the local contribution to the right hand side is given by

$$(23) \quad b_h^P(f, v_h) = b^P(\Pi_k^0 f, v_h) \quad \forall v_h \in V_h^k(P), \quad \forall P \in \mathcal{T}_h.$$

With the above definitions, the discrete source problem is well-posed and its solution converges to the continuous one with optimal order, (see [5, 2]): there exists a positive constant  $C$ , independent of  $h$  such that

$$(24) \quad \|u - u_h\|_1 \leq C \left( |u - u_I|_1 + |u - u_\pi|_{1,h} + \sup_{v_h \in V_h^k} \frac{|b(f, v_h) - b_h(f, v_h)|}{|v_h|_1} \right),$$

where  $u_I \in V_h^k$  and  $u_\pi$  are defined in Proposition 3. We observe that the last term in (24) is a consistency term in the spirit of the *first Strang Lemma* [21, Th. 4.1.1]. Indeed, the VEM discretization provides a conforming discrete subspace of  $V$ , but the bilinear forms  $a_h$  and  $b_h$  differ from the continuous ones. The consistency error generated by the difference between  $a$  and  $a_h$  is already incorporated in the first two terms on the right hand side of (24), while the one related to  $b$  depends on the properties of the source term  $f$ . In particular, if  $f \in L^2(\Omega)$  we obtain that the error converges to zero with optimal order depending on the regularity of the solution  $u$ :

$$\|u - u_h\|_1 \leq C (h^r |u|_{1+r} + h \|f\|_0).$$

We now turn to the virtual element discretization of the eigenvalue problem (1). Let us recall the discrete formulation: find  $(\lambda_h, u_h) \in \mathbb{R} \times V_h^k$  with  $u_h \neq 0$  such that

$$(25) \quad a_h(u_h, v_h) = \lambda_h b_h(u_h, v_h) \quad \forall v_h \in V_h^k,$$

where, using definition (23)

$$(26) \quad b_h^P(u_h, v_h) = b^P(\Pi_k^0 u_h, v_h) = b^P(\Pi_k^0 u_h, \Pi_k^0 v_h).$$

The following generalized algebraic eigenvalue problem corresponds to the discrete eigenvalue problem:

$$(27) \quad \mathbf{A}u = \lambda_h \mathbf{M}u,$$

where  $\mathbf{A}$  and  $\mathbf{M}$  are the  $N_h \times N_h$  matrices associated with the bilinear forms  $a_h$  and  $b_h$ , respectively.

As observed for the form  $a_h^P$ , it might happen that  $\Pi_k^0 u_h = 0$  for a non vanishing  $u_h$  and thus  $b_h^P(u_h, v_h) = 0$  for all  $v_h \in V_h^k$ . This means that the local contribution to the matrix  $\mathbf{M}$  has a non trivial kernel similarly to what we have observed for the form  $a_h^P$  and some components of  $V_h^k$  may not be controlled by the global mass matrix. It is then natural to add a stabilization term as follows:

$$(28) \quad b_h^P(u_h, v_h) = b^P(\Pi_k^0 u_h, \Pi_k^0 v_h) + S_b^P((I - \Pi_k^0)u_h, (I - \Pi_k^0)v_h),$$

where  $S_b^P$  is a symmetric positive definite bilinear form defined on  $V_h^k(P) \times V_h^k(P)$  scaling as  $b^P(\cdot, \cdot)$ , that is there exist two positive constants  $\beta_*$  and  $\beta^*$  such that

$$(29) \quad \beta_* b^P(v_h, v_h) \leq S_b^P(v_h, v_h) \leq \beta^* b^P(v_h, v_h) \quad \forall v_h \in V_h^k(P), \quad \forall P \in \mathcal{T}_h.$$

*Remark 2.* It is out of the aims of this paper to discuss the choice of algorithms for the solution of the algebraic eigenvalue problem  $\mathbf{A}u = \lambda \mathbf{M}u$ . Nevertheless, the presence of the stabilizing parameters may influence such choice. For instance, if the matrix  $\mathbf{M}$  is singular and  $\mathbf{A}$  is not, then it might be convenient to solve the reciprocal system  $\mathbf{M}u = \lambda^{-1} \mathbf{A}u$ . The definition itself of solution for problems like this can be difficult to give, in particular, when both  $\mathbf{A}$  and  $\mathbf{M}$  are singular and their kernels have a non trivial intersection. On the other hand if  $u$  belongs to the kernel of  $\mathbf{M}$  and not to that of  $\mathbf{A}$ , we may conventionally say that it is an eigenfunction corresponding to the eigenvalue  $\lambda = \infty$ .

From now on, unless explicitly stated, we shall consider the discrete eigenvalue problem (25) with the local form  $b_h^P$  defined as in (28).

**3.3. Convergence analysis.** In this section we show the convergence of the discrete eigenpairs to the continuous ones by applying Theorem 1 and prove a priori error estimates.

In order to apply Theorem 1 we need to prove  $L^2$ -error estimates for the source problems (2) and (6). For the sake of completeness, we report here the proof.

**Theorem 4.** *Given  $f \in L^2(\Omega)$ , let  $u \in H_0^1(\Omega)$  and  $u_h \in V_h^k$  denote the solutions to (2) and to (6), respectively. Then there exists a constant  $C$  independent of  $h$  such that*

$$(30) \quad \|u - u_h\|_0 \leq Ch^t \left( |u - u_I|_1 + |u - u_\pi|_{1,h} + \|f - \Pi_k^0 f\|_0 \right),$$

where  $t = \min(r, 1)$ , being  $r$  the regularity index of the solution  $u$ , see (13) and  $u_I$  and  $u_\pi$  are defined in Proposition 3.

*Proof.* We use a duality argument and denote by  $\psi \in H_0^1(\Omega)$  the solution to

$$(31) \quad a(\psi, v) = b(u - u_h, v) \quad \forall v \in H_0^1(\Omega).$$

Since  $u - u_h \in L^2(\Omega)$ , then  $\psi \in H^{1+r}(\Omega)$  with  $\|\psi\|_{1+r} \leq C\|u - u_h\|_0$ . Let  $\psi_I \in V_h^k$  be the interpolant of  $\psi$  given by Proposition 3, then for  $t = \min(r, 1)$  it holds

$$(32) \quad \|\psi - \psi_I\|_0 + h|\psi - \psi_I|_1 \leq Ch^{1+t}\|u - u_h\|_0.$$

We have that

$$(33) \quad \begin{aligned} \|u - u_h\|_0^2 &= b(u - u_h, u - u_h) = a(u - u_h, \psi) \\ &= a(u - u_h, \psi - \psi_I) + a(u - u_h, \psi_I) = I + II. \end{aligned}$$

We first estimate the term  $I$  as follows

$$(34) \quad I = a(u - u_h, \psi - \psi_I) \leq C(|u - u_h|_1 h^t \|u - u_h\|_0).$$

Then

$$\begin{aligned} II &= a(u - u_h, \psi_I) = b(f, \psi_I) - a_h(u_h, \psi_I) + a_h(u_h, \psi_I) - a(u_h, \psi_I) \\ &= [b(f, \psi_I) - b_h(f, \psi_I)] + [a_h(u_h, \psi_I) - a(u_h, \psi_I)] \\ &= III + IV. \end{aligned}$$

We have that

$$(35) \quad III = \sum_P \left( b^P(f, \psi_I) - b^P(\Pi_k^0 f, \Pi_k^0 \psi_I) - S_b^P((I - \Pi_k^0)f, (I - \Pi_k^0)\psi_I) \right).$$

It holds

$$(36) \quad \begin{aligned} b^P(f, \psi_I) - b^P(\Pi_k^0 f, \Pi_k^0 \psi_I) &= b^P(f - \Pi_k^0 f, \psi_I - \Pi_k^0 \psi_I) \\ &\leq Ch^t \|f - \Pi_k^0 f\|_0 \|u - u_h\|_0 \end{aligned}$$

and

$$(37) \quad \begin{aligned} S_b^P((I - \Pi_k^0)f, (I - \Pi_k^0)\psi_I) &\leq \beta^* \|(I - \Pi_k^0)f\|_0 \|(I - \Pi_k^0)\psi_I\|_0 \\ &\leq Ch^t \|(I - \Pi_k^0)f\|_0 \|u - u_h\|_0. \end{aligned}$$

Finally, estimating the term  $IV$  with standard VEM argument, we obtain

$$IV \leq C \left( \|u - u_h\|_1 + \|u - \Pi_k^0 u\|_{1,h} \right) h^t \|u - u_h\|_0.$$



Putting together all the estimates, we conclude the proof.  $\square$

The  $L^2$ -error estimate proved above implies the uniform convergence stated in Theorem 1.

**Theorem 5.** *Let  $T_h$  and  $T$  be the families of operators associated with problems (6) and (2), respectively. Then the following uniform convergence holds true:*

$$\|T - T_h\|_{\mathcal{L}(L^2(\Omega), L^2(\Omega))} \rightarrow 0 \quad \text{for } h \rightarrow 0.$$

*Proof.* Given  $f \in L^2(\Omega)$ , let  $Tf$  and  $T_h f$  be the solutions to problems (2) and (6), respectively. Then, using the  $L^2$ -estimate of Theorem 4, the interpolation and approximation results in Proposition 3, and the stability condition (13), we obtain

$$\|Tf - T_h f\|_0 \leq Ch^t \|f\|_0,$$

where  $t = \min(k, r)$ ,  $k \geq 1$  is the order of the method,  $r$  the regularity exponent in (13), and  $C$  a constant independent of  $f$  and  $h$ . From this inequality it follows that

$$\|T - T_h\|_{\mathcal{L}(L^2(\Omega), L^2(\Omega))} = \sup_{f \in L^2(\Omega)} \frac{\|Tf - T_h f\|_0}{\|f\|_0} \leq Ch^t,$$

which implies the uniform convergence.  $\square$

We now turn to error estimates for the approximation of the eigenvalues and the eigenfunctions. First of all we state a result on the rate of convergence for the solutions to the source problems when  $f$  is smooth.

**Proposition 6.** *Assume that  $f \in H^{1+s_1}(\Omega)$  and that the solution  $u$  of problem (2) belongs to  $H^{1+s_2}(\Omega)$  for some  $s_1$  and  $s_2$  greater than 0, then the estimate (30) implies*

$$(38) \quad \|u - u_h\|_0 \leq Ch^t \left( h^{\min(k, s_2)} |u|_{1+s_2} + h^{1+\min(k, s_1)} |f|_{1+s_1} \right)$$

where  $t = \min(1, r)$ .

*Remark 3.* We point out that an eigenfunction  $u$  can be seen as the solution of a source problem with right hand side equal to  $\lambda u$ , which belongs at least to  $H_0^1(\Omega)$ . Hence the second term in the right side of (38) is at least of first order. In general, if the domain is non convex, the solution  $u$  to (2) belongs at least to  $H^{1+r}(\Omega)$  with  $r \in (\frac{1}{2}, 1]$ , even if the right hand side is more regular, see (13). However, it might happen that  $u$  is more regular, for example that it belongs to the space  $H^{1+s}(\Omega)$  with  $s \geq r$ , then estimate (38) reduces to

$$(39) \quad \|u - u_h\|_0 \leq Ch^{t+\min(k, s)} |u|_{1+s}.$$

Taking into account the above  $L^2$ -estimates and using the abstract Theorem 2, we obtain the optimal rate of convergence for the approximation of the eigenpairs.

**Theorem 7.** *Let  $\lambda_i$  be an eigenvalue of problem (1), with multiplicity  $m$  (that is  $\lambda_i = \dots = \lambda_{i+m-1}$ ) and let  $\mathcal{E}_i$  be the corresponding eigenspace. We assume that all the elements in  $\mathcal{E}_i$  belong to  $H^{1+s}(\Omega)$  for some  $s \geq r$  (see (13)). Moreover, let  $\mathcal{E}_{i,h} = \bigoplus_{j=i}^{i+m-1} \text{span}(u_{h,j})$ , where  $u_{h,j}$  is the discrete eigenfunction associated with  $\lambda_{h,j}$ . Then, for  $h$  small enough, there exists a constant  $C$  independent of  $h$  such that*

$$(40) \quad \delta(\mathcal{E}_i, \mathcal{E}_{i,h}) \leq Ch^{t+\min(k, s)}$$

with  $t = \min(1, r)$ .

*Proof.* The result directly stems from (9). Indeed,

$$(41) \quad \delta(\mathcal{E}_i, \mathcal{E}_{i,h}) \leq C \|(T - T_h)|_{\mathcal{E}_i}\|_{\mathcal{L}(L^2(\Omega), L^2(\Omega))} = C \sup_{\substack{u \in \mathcal{E}_i \\ \|u\|_0=1}} \|(T - T_h)u\|_0.$$

Since  $u \in \mathcal{E}_i$ , it holds that  $u \in H^{1+s}(\Omega)$  with  $\|u\|_{1+s} \leq C\|u\|_0$  (see (13)). Hence the result follows from estimate (39).  $\square$

Now we state the *a priori* error estimates for the eigenvalues.

**Theorem 8.** *Using the notation of Theorem 7, there exists a constant  $C$  independent of  $h$ , but depending on  $\lambda_i$  such that the following error estimate for the eigenvalues holds true:*

$$|\lambda_j - \lambda_{j,h}| \leq Ch^{2\min(k,s)} \quad \text{for } j = i, \dots, i + m - 1.$$

*Proof.* We apply Theorem 2. Thanks to (41), it remains to bound the first term in (10). This is equivalent to estimate  $b((T - T_h)w, z)$  for all  $w$  and  $z$  in  $\mathcal{E}_i$ . After some computations we get

$$\begin{aligned} b((T - T_h)w, z) &= a(Tz, (T - T_h)w) \\ &= a((T - T_h)z, (T - T_h)w) + b(T_h z, w) - b_h(T_h z, w) \\ &\quad - a(T_h z, T_h w) + a_h(T_h z, T_h w) \\ &= I' + II' + III'. \end{aligned}$$

We estimate separately the three terms. It is straightforward to obtain

$$(42) \quad I' \leq \|(T - T_h)z\|_1 \|(T - T_h)w\|_1 \leq Ch^{2\min(k,s)}.$$

In order to estimate the second term, we proceed as in (35) by writing it as a sum over the elements  $P \in \mathcal{T}_h$ ,

$$(43) \quad \begin{aligned} II' &= \sum_P \left( b^P(T_h z - \Pi_k^0(T_h z), w - \Pi_k^0 w) - S_b^P((I - \Pi_k^0)T_h z, (I - \Pi_k^0)w) \right) \\ &\leq C \sum_P \|(I - \Pi_k^0)T_h z\|_{0,P} \|I - \Pi_k^0 w\|_{0,P} \leq Ch^{2\min(k,s)}. \end{aligned}$$

Finally,

$$(44) \quad \begin{aligned} III' &= \sum_P \left( a_h^P(T_h z - \Pi_k^0 Tz, T_h w - \Pi_k^0 Tw) - a^P(T_h z - \Pi_k^0 Tz, T_h w - \Pi_k^0 Tw) \right) \\ &\leq C \sum_P \left( |T_h z - Tz|_{1,P} + |(I - \Pi_k^0)Tz|_{1,P} \right) \\ &\quad \left( |T_h w - Tw|_{1,P} + |(I - \Pi_k^0)Tw|_{1,P} \right) \leq Ch^{2\min(k,s)}. \end{aligned}$$

Collecting estimates (42)-(44) yields the required estimate.  $\square$

Bearing in mind Remark 1, we state the rate of convergence for the error in the approximation of the eigensolutions with respect to the  $H^1$ -norm. To this aim we denote by  $\delta_1(E, F)$  the gap between the spaces  $E$  and  $F$  measured in the  $H^1$ -norm.

**Theorem 9.** *Using the same notation as in Theorem 7, and assuming that all the elements in  $\mathcal{E}_i$  belong to  $H^{1+s}(\Omega)$  for some  $s \geq r$ , then for  $h$  small enough, there exists a constant  $C$  independent of  $h$  such that*

$$\delta_1(\mathcal{E}_i, \mathcal{E}_{i,h}) \leq Ch^{\min(k,s)}.$$

*Remark 4.* The above analysis has been carried on considering the stabilized discrete bilinear form  $b_h$ , whose local counterpart is given in (28). However, in [26] it has been shown that the results stated in Theorems 7-9 hold true also when  $b_h$  is defined using the *non-stabilized* local version in (26).

**3.4. Numerical results.** Here and in the following sections devoted to the numerical experiments, we focus on the solution to problem (11) on a square and an *L-shaped* domain. It is well known that in the first test case the eigenfunctions are analytic, while in the latter they can be singular due to the presence of a reentrant corner in the domain. All the results that we are going to present are not new, including the figures which have been already published in [26, 25, 36].

The implementation of the method requires a precise definition for the stabilization terms. Here we are going to consider one possible choice, other possibilities are reported in [26]. For  $v_h$  and  $w_h$  in  $V_h^k(P)$ , the stabilizing bilinear forms  $S_a^P(v_h, w_h)$  and  $S_b^P(v_h, w_h)$  (see (20) and (28)) are defined using the local degrees of freedom associated to  $V_h^k(P)$ . Let  $N_P$  be the dimension of  $V_h^k(P)$ , then  $\mathbf{v}$  and  $\mathbf{w}$  stand for the vectors in  $\mathbb{R}^{N_P}$  with components the local degrees of freedom associated to  $v_h$  and  $w_h$ . More precisely, we set

$$(45) \quad S_a^P(v_h, w_h) = \alpha_P \mathbf{v}^\top \mathbf{w} \quad \text{and} \quad S_b^P(v_h, w_h) = \beta_P h_P^2 \mathbf{v}^\top \mathbf{w},$$

where  $\alpha_P$  and  $\beta_P$  are constants independent of  $h$ . The numerical results we report here are obtained choosing  $\alpha_P$  as the mean value of the eigenvalues of the local matrix associated to the consistency term  $a^P(\Pi_k^\nabla v_h, \Pi_k^\nabla w_h)$ . The parameter  $\beta_P$  is given by the mean value of the eigenvalues of the local mass matrix associated to  $\frac{1}{h_P^2} b^P(\Pi_k^0 v_h, \Pi_k^0 w_h)$ . With this definition  $\alpha_P$  and  $\beta_P$  depend only on the shape of  $P$ .

**Square domain** Let  $\Omega$  be the square  $(0, \pi)^2$ , then the eigensolutions of (11) are given by

$$(46) \quad \begin{aligned} \lambda_{i,j} &= (i^2 + j^2) \quad \text{for } i, j \in \mathbb{N}, \text{ with } i, j \neq 0 \\ u_{i,j}(x, y) &= \sin(ix) \sin(jy) \quad \text{for } (x, y) \in \Omega. \end{aligned}$$

We consider different refinements of a *Voronoi* mesh, an example of them is shown in Figure 1 left. Figure 2 reports the error for the first six eigenvalues obtained with different polynomial degrees  $k = 1, 2, 3, 4$  on meshes with size  $h = \frac{\pi}{8}, \frac{\pi}{16}, \frac{\pi}{32}, \frac{\pi}{64}$ . The slopes of the lines corresponding to the error for each eigenvalue clearly reflects the theoretical rate of convergence stated in Theorem 8. For  $k = 4$  the error is close to the machine precision for the two last refinements, therefore the effect of propagation of rounding error prevents further decreasing. Remark 4 points out that the stabilization on the right hand side is not necessary at the theoretical level. In order to understand if it might impact the numerical results, we report in Table 1 a comparison between the errors obtained using the stabilized or non-stabilized bilinear form  $b_h$ , corresponding to the first four distinct eigenvalues for  $k = 1$  and  $k = 4$ . It might be appreciated that the magnitude of the error is actually the same. A more detailed discussion on the role of the stabilizing parameters will be performed in Section 5.

**L-shaped domain** The Laplace eigenvalue problem with Neumann boundary conditions on the non convex L-shaped domain  $\Omega = (-1, 1)^2 \setminus (0, 1) \times (-1, 0)$  (displayed in Figure 1 right with an example of the used Voronoi mesh) is a well-known benchmark test to check the capability of the numerical scheme to approximate

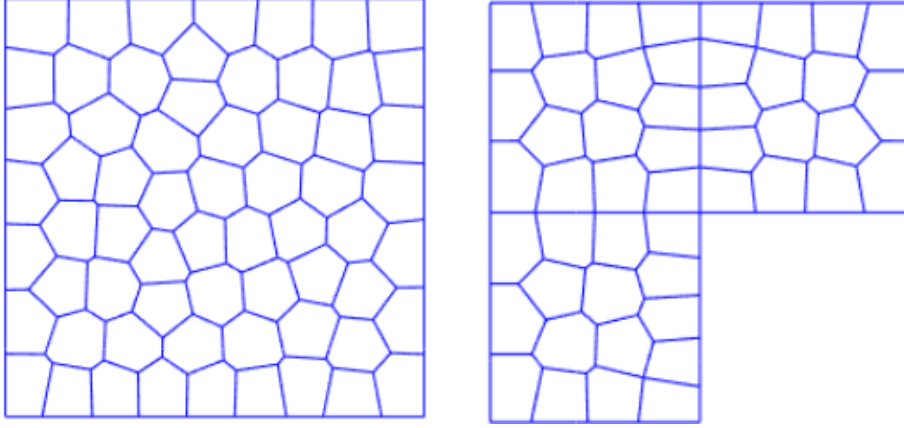


FIGURE 1. Examples of Voronoi mesh of the unit square and the L-shaped domain

$k = 1$									
$h$	$\lambda_1 = 2$		$\lambda_2 = 5$		$\lambda_4 = 8$		$\lambda_5 = 10$		
	stab	non stab	stab	non stab	stab	non stab	stab	non stab	
$\pi/8$	$1.654e-2$	$1.766e-2$	$3.650e-2$	$4.098e-2$	$5.196e-2$	$6.384e-2$	$7.107e-2$	$8.488e-2$	
$\pi/16$	$4.418e-3$	$4.611e-3$	$9.578e-3$	$1.026e-2$	$1.446e-2$	$1.558e-2$	$1.758e-2$	$1.926e-2$	
$\pi/32$	$8.206e-4$	$8.784e-4$	$2.320e-3$	$2.465e-3$	$3.768e-3$	$4.003e-3$	$4.715e-3$	$5.038e-3$	
$\pi/64$	$1.662e-4$	$1.808e-4$	$5.289e-4$	$5.663e-4$	$8.722e-4$	$9.340e-4$	$9.643e-4$	$1.042e-3$	
$k = 4$									
$h$	$\lambda_1 = 2$		$\lambda_2 = 5$		$\lambda_4 = 8$		$\lambda_5 = 10$		
	stab	non stab	stab	non stab	stab	non stab	stab	non stab	
$\pi/8$	$4.087e-08$	$4.094e-08$	$3.033e-06$	$3.046e-06$	$7.856e-06$	$7.915e-06$	$4.428e-05$	$4.470e-05$	
$\pi/16$	$8.101e-11$	$8.098e-11$	$8.329e-09$	$8.340e-09$	$4.364e-08$	$4.373e-08$	$1.475e-07$	$1.475e-07$	
$\pi/32$	$6.451e-10$	$6.449e-10$	$2.109e-12$	$1.283e-12$	$1.062e-10$	$1.060e-10$	$2.211e-10$	$2.223e-10$	
$\pi/64$	$6.541e-10$	$6.542e-10$	$8.818e-11$	$8.829e-11$	$3.815e-10$	$3.817e-10$	$1.706e-10$	$1.707e-10$	

TABLE 1. Comparison of the errors for the first eigenvalues between stabilized and non stabilized bilinear form  $b_h$

singular eigensolutions. The analysis presented above for the Dirichlet eigenvalue problem extends analogously to this situation. In Figure 3, we show the convergence history for the first and the third eigenvalues computed with  $k = 1, 2, 3$  and the stabilization parameter chosen as in (45). The reference value for the eigenvalues has been taken from the benchmark solution set [22]. Due to the presence of the reentrant corner, the first eigensolution is singular belonging to  $H^{1+r}(\Omega)$  with  $r = 2/3 - \varepsilon$ , hence the rate of convergence for the first eigenvalue results to be  $4/3$ . On the other hand, the third eigenfunction is analytic and the scheme provides the correct  $O(h^{2k})$  rate of convergence.

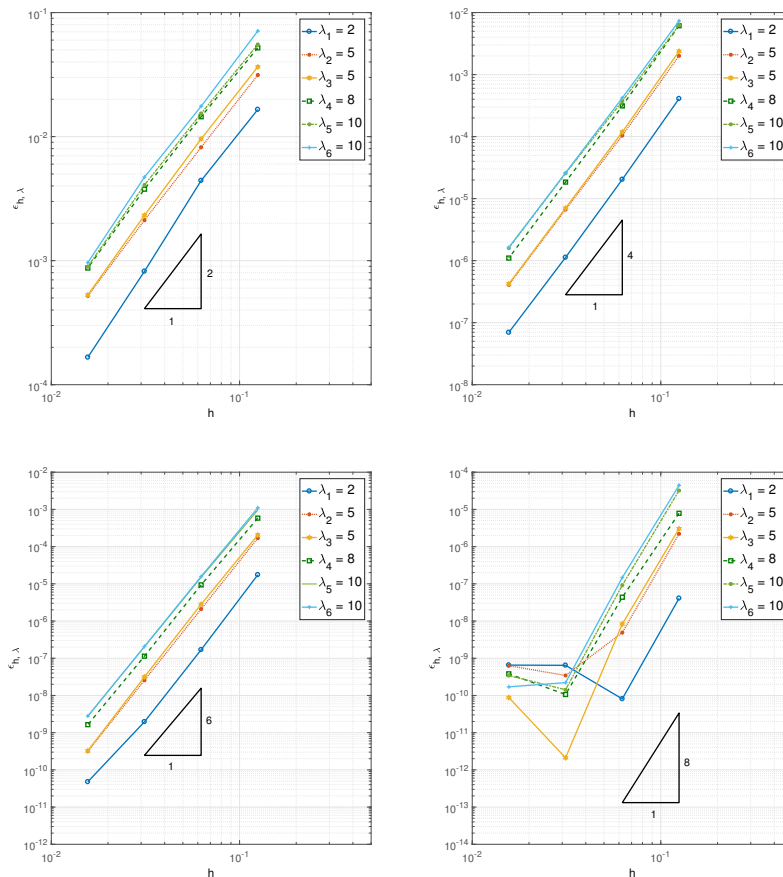


FIGURE 2. Rate of convergence for the first six eigenvalues on the square domain. Top left:  $k = 1$ , top right:  $k = 2$ , bottom left:  $k = 3$ , bottom right:  $k = 4$

#### 4. EXTENSION TO NONCONFORMING AND $hp$ VERSION OF VEM

This section is devoted to the presentation of the nonconforming,  $p$  and  $hp$  versions of the discrete virtual space and reports the main results relative to the approximation of the eigenvalue problem. In particular, we are going to report on the results of [25, 36].

**4.1. Nonconforming VEM.** We start by treating the nonconforming case following [25]. We introduce the broken Sobolev space

$$H_h^s = \{v \in L^2(\Omega) : v|_P \in H^s(P) \forall P \in \mathcal{T}_h\}$$

and the corresponding broken norm

$$\|v\|_{s,h} = \left( \sum_{P \in \mathcal{T}_h} \|v\|_{s,P}^2 \right)^{\frac{1}{2}}.$$

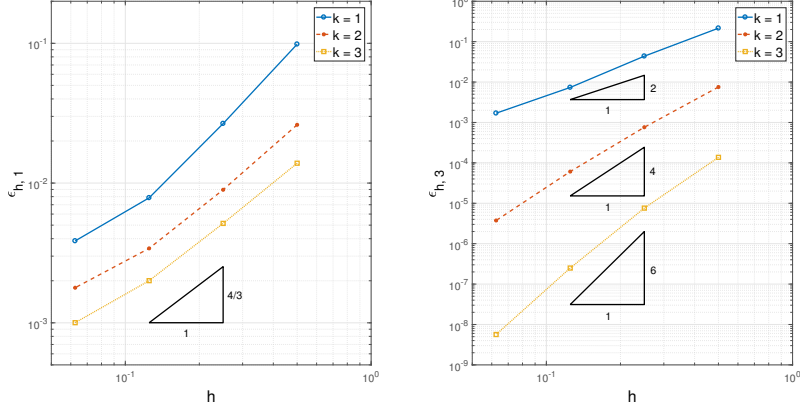


FIGURE 3. Rate of convergence for the first eigenvalue (left) and the third one (right) on the L-shaped domain

With the aim of constructing the nonconforming space, we need some definitions. Let  $P^+$  and  $P^-$  be two elements sharing the edge  $e$  and  $\mathbf{n}_e^\pm$  the outward unit normal vector to  $\partial P^\pm$ . The jump of  $v$  across any internal edge  $e$  is  $[[v]] = v^+ \mathbf{n}_e^+ + v^- \mathbf{n}_e^-$ , where  $v^\pm$  is the restriction of  $v$  to  $P^\pm$ . If  $e \in \mathcal{E}_h^\partial$  we set  $[[v]] = v_e \mathbf{n}_e$ .

The construction of the nonconforming virtual element space is based on a different definition of the local space  $V_h^k(P)$ . More precisely, instead of imposing that the functions have a continuous trace along the element boundary, we prescribe the normal derivative on each edge of  $P$  to be a polynomial of degree  $k-1$ , that is  $V_h^k(P)$  is given by (14) and (15) with

$$(47) \quad \tilde{V}_h^k(P) = \left\{ v_h \in H^1(P) : \frac{\partial v_h}{\partial \mathbf{n}} \in \mathbb{P}_{k-1}(P) \forall e \subset \partial P, \Delta v_h \in \mathbb{P}_k(P) \right\}.$$

The degrees of freedom are given by the moments of  $v_h$  of order up to  $k-1$  on each edge  $e$  of  $P$  and the moments up to order  $k-2$  on  $P$ . As in the conforming case,  $\Pi_k^\nabla v_h$  can be exactly evaluated by means of these degrees of freedom.

The *global nonconforming virtual element space* is then defined for,  $k \geq 1$ , as

$$(48) \quad V_h^{k,nc} = \{ v_h \in H^{1,nc}(\mathcal{T}_h; k) : v_h|_P \in V_h^k(P) \forall P \in \mathcal{T}_h \},$$

where as in the finite element framework,

$$(49) \quad H^{1,nc}(\mathcal{T}_h; k) = \left\{ v \in H_h^1 : \int_e [[v]] \cdot \mathbf{n}_e p ds = 0 \forall p \in \mathbb{P}_{k-1}(e), \forall e \in \mathcal{E}_h \right\},$$

being  $\mathbf{n}_e$  the outward normal unit vector to  $e$  with orientation fixed once and for all. It is clear that  $V_h^{k,nc}$  is not a subspace of  $H_0^1(\Omega)$ , this will imply that in the error analysis we have to take into account a *consistency error*.

Proposition 3 still holds true with  $v_I$  being the interpolant of  $v$  constructed using the above degrees of freedom, see for example [20].

The discrete eigenvalue problem reads: find  $(\lambda_h, u_h) \in \mathbb{R} \times V_h^{k,nc}$  with  $u_h \neq 0$  such that

$$(50) \quad a_h(u_h, v_h) = \lambda_h b_h(u_h, v_h) \quad \forall v_h \in V_h^{k,nc},$$

where the bilinear forms  $a_h$  and  $b_h$  are defined in (20) and in (28). We recall also the discrete source problem: given  $f \in L^2(\Omega)$  find  $u_h \in V_h^{k,nc}$  such that

$$(51) \quad a_h(u_h, v_h) = b_h(f, v_h) \quad \forall v_h \in V_h^{k,nc}.$$

We define, as usual, the resolvent operator  $T_h : L^2(\Omega) \rightarrow L^2(\Omega)$  with  $T_h f = u_h \in V_h^{k,nc}$  solution to (51). We notice that in this case  $T_h$  cannot be defined with range in  $H_0^1(\Omega)$ , therefore we shall obtain a result similar to Theorem 9 with the gap measured in the broken  $H^1$ -norm.

The analysis of the nonconforming case can be carried on with the same arguments used in the conforming case, stemming from the broken  $H^1$ -norm estimate for the error of the solution of the source problem. We start with the following result proved in [3]: there exists a positive constant  $C$  independent of  $h$  such that

$$(52) \quad \|u - u_h\|_{1,h} \leq C \left( |u - u_I|_{1,h} + |u - u_\pi|_{1,h} + \sup_{v_h \in V_h^{k,nc}} \frac{|b(f, v_h) - b_h(f, v_h)|}{|v_h|_{1,h}} + \sup_{v_h \in V_h^{k,nc}} \frac{\mathcal{R}_h(u, v_h)}{|v_h|_{1,h}} \right),$$

where

$$(53) \quad \mathcal{R}_h(u, v_h) = \sum_{P \in \mathcal{T}_h} a^P(u, v_h) - b(f, v_h) = \sum_{e \in \mathcal{E}_h^0} \int_e \nabla u \cdot \llbracket v_h \rrbracket ds.$$

The term  $\mathcal{R}_h(u, v_h)$  represents an additional *consistency error* which, in the spirit of the *second Strang Lemma* [21, Th. 4.2.2], is due to the fact that the discrete functions are not continuous across inter-element edges. With standard arguments using the degrees of freedom of the nonconforming virtual elements on the element boundary and a Poincaré inequality (see [16]), one can prove that for  $u \in H^{1+r}(\Omega)$ , with  $r > 1/2$ ,

$$(54) \quad \mathcal{R}_h(u, v_h) \leq Ch^r \|u\|_{1+r} |v_h|_{1,h} \quad \forall v_h \in V_h^{k,nc}.$$

In order to obtain the uniform convergence of  $T_h$  to  $T$ , we first show the  $L^2$ -error estimate for the solution to the source problem.

**Theorem 10.** *Let  $f \in L^2(\Omega)$ ,  $u \in H_0^1(\Omega)$  and  $u_h \in V_h^{k,nc}$  be the solutions to (2) and (51), respectively. Then there exists a constant  $C$ , independent of  $h$ , such that for  $t = \min(1, r)$*

$$(55) \quad \|u - u_h\|_0 \leq Ch^t \left( |u - u_h|_{1,h} + |u - u_\pi|_{1,h} + \|f - \Pi_k^0 f\|_0 + \sup_{v_h \in V_h^{k,nc}} \frac{\mathcal{R}_h(u, v_h)}{|v_h|_{1,h}} \right).$$

*Proof.* The proof follows the same lines as that of Theorem 4. We have to take into account the consistency error. Let  $\psi \in H_0^1(\Omega)$  be the solution to (31), then we have

$$\|u - u_h\|_0^2 = \sum_P (a^P(u - u_h, \psi - \psi_I) + a^P(u - u_h, \psi_I)) + \mathcal{R}_h(\psi, u_h).$$

Thanks to (34) and (54), it remains to estimate the second term in the sum, which can be split as follows:

$$\begin{aligned} \sum_P a^P(u, \psi_I) &= b(f, \psi_I) + \mathcal{R}_h(u, \psi_I) \\ \sum_P a^P(u_h, \psi_I) &= b_h(f, \psi_I) + \sum_P (a^P(u_h, \psi_I) - a_h^P(u_h, \psi_I)). \end{aligned}$$

We use again (54) and observe that the other terms can be estimated as the terms III and IV in the proof of Theorem 4. Putting together all the estimates yields the required bound.  $\square$

Assuming that  $f \in H^{1+s_1}(\Omega)$  and that the solution  $u$  to problem (2) belongs to  $H^{1+s_2}(\Omega)$  for some  $s_1 > 0$  and  $s_2 > \frac{1}{2}$ , then we obtain again the bound (38). This optimal rate of convergence yields the rate convergence for the gap between the eigenspaces and for the eigenvalue error as in Theorems 7 and 8. The analogous result as the one in Theorem 9 can be obtained if the gap is measured using the broken  $H^1$ -norm.

Numerical results confirming the theory are presented in [25] where the domain is a square or L-shaped. The nonconforming VEM has been tested on four different types of meshes including also non convex elements providing always optimal rate of convergence in the case of analytic eigenfunctions. In particular, in [25] a comparison of the rate of convergence between conforming and nonconforming approximation has been presented showing very close behavior. The benchmark with the L-shaped domain has been also considered and again the results agree with those presented in Figure 3.

**4.2.  $hp$  version of VEM.** Let us now recall briefly the  $p$  and  $hp$  version of the virtual element method and show how these methods can be applied to the discretization of the eigenvalue problem. We refer, in particular, to [36] although we are considering the simpler model problem (11), and to [7] for the basic principles of  $hp$  virtual elements.

In this case the spaces we are considering, are labeled with a subindex  $n \in \mathbb{N}$  and refer to conforming polygonal decompositions of  $\Omega$  denoted by  $\mathcal{T}_n$ . Given an element  $P \in \mathcal{T}_n$  and the polynomial degree  $p \in \mathbb{N}$ ,  $V_n^p(P)$  is the local virtual space and coincides with the space  $V_h^k(P)$ , with the due changes in the notation. Hence the global space  $V_n^p$  is the subspace of  $H_0^1(\Omega)$  defined as  $V_n^p = \{v_n \in H_0^1(\Omega) : v_n|_P \in V_n^p(P) \forall P \in \mathcal{T}_n\}$ . Analogously, we shall use the subindex  $n$  instead of  $h$  in all the definitions involving discrete quantities.

The results of approximation in the space  $V_n^p$  are similar to those in Proposition 3, but trace the dependence on the degree  $p$ , so that the exponential convergence of the error can be deduced.

**Proposition 11.** *Given  $P \in \mathcal{T}_n$  and  $u \in H^{1+s}(P)$ ,  $s > 0$ , for all  $p \in \mathbb{N}$ , there exists  $u_\pi \in \mathbb{P}_p(P)$  and a constant  $C$  independent of  $p$ , such that*

$$|u - u_\pi|_{\ell, P} \leq C \frac{h_P^{1+\min(p,s)-\ell}}{p^{1+s-\ell}} \|u\|_{1+s, P} \quad \text{for } 0 \leq \ell \leq s.$$



Moreover, given  $u \in H_0^1(\Omega)$  with  $u|_P \in H^{1+s}(P)$  for all  $P \in \mathcal{T}_n$  and for some  $s \geq 1$ , there exists  $u_I \in V_n^p$  such that

$$|u - u_I|_1 \leq C \frac{h^{\min(p,s)}}{p^{s-1}} \left( \sum_{P \in \mathcal{T}_n} \|u\|_{1+s,P}^2 \right)^{\frac{1}{2}}.$$

We point out that the use of high degree  $p$  is convenient in the approximation of smooth (piecewise smooth) functions.

The approximation of the eigenvalue problem (11) can be written introducing the local discrete bilinear forms already used in the  $h$ -conforming case (20) and (28). Then the discrete eigenvalue problem reads: find  $(\lambda_n, u_n) \in \mathbb{R} \times V_n^p$  with  $u_n \neq 0$  such that

$$(56) \quad a_n(u_n, v_n) = \lambda_n b_n(u_n, v_n) \quad \forall v_n \in V_n^p.$$

As it is standard for eigenvalue problems, we associate the discrete source problem: given  $f \in L^2(\Omega)$  find  $u_n \in V_n^p$  such that

$$(57) \quad a_n(u_n, v_n) = b_n(f, v_n) \quad \forall v_n \in V_n^p.$$

In order to take advantage of the approximation properties listed in Proposition 11, we define the resolvent operator  $T$  on  $H^1(\Omega)$  in the spirit of Remark 1. Hence for  $f \in H^1(\Omega)$ ,  $Tf = u$  is the solution to the continuous source problem (2), while in the discrete case,  $T_n f = u_n \in V_n^p$  stands for the solution to (57).

The convergence of eigensolutions derives from the uniform convergence of  $T_n$  to  $T$ , which in turn is a consequence of the error estimates for the source problem.

**Theorem 12.** *Given  $f \in H^1(\Omega)$ , let  $u \in H_0^1(\Omega)$  and  $u_n \in V_n^p$  be the solutions to (2) and (57), respectively. Assume that the restrictions of  $f$  and  $u$  to every element  $P \in \mathcal{T}_n$  belong to  $H^{1+s}(P)$  for some  $s \geq 0$ , then there exists a constant  $C$  independent of  $h$  and  $p$  such that*

$$|u - u_n|_1 \leq C \frac{h^{\min(p,s)}}{p^{s-1}} (h^2 \|f\|_{1+s,n} + \|u\|_{1+s,n}).$$

For the proof it is enough to combine Proposition 11 with standard VEM arguments. In [36], a precise dependence of  $C$  on the ellipticity constant of the form  $a$  and the constants in (21), and (29) is obtained. In particular, it is shown that the constants in (21) and (29) might depend on  $p$ , as we shall see later.

The result in Theorem 12, together with the arguments of [7, Section 5], yields the following exponential convergence:

**Theorem 13.** *Let  $u$  and  $u_n$  be as in Theorem 12, and assume that  $u$  is the restriction on  $\Omega$  of an analytic function defined on an extension of  $\Omega$ . Then there exist two positive constants  $C$  and  $c$  independent of the discretization parameters such that*

$$|u - u_n|_1 \leq C \exp(-cp).$$

Theorem 12 implies the uniform convergence of  $\|T - T_n\|_{\mathcal{L}(H^1(\Omega), H^1(\Omega))}$  to zero, more precisely one can show that under the same assumptions as in Theorem 13 it holds true:

$$\|T - T_n\|_{\mathcal{L}(H^1(\Omega), H^1(\Omega))} \leq C \exp(-cp).$$

Then, applying Theorems 8 and 9, we obtain the spectral convergence both for the error in the approximation of the eigenvalues, and the gap between the continuous

and the discrete eigenspaces, provided the eigenfunctions are analytic. For the details, we refer to [36]. Figure 4 shows the convergence of the  $p$ -version of VEM in comparison with the  $h$ -version with fixed  $p = 1, 2, 3$  for the test case on the square  $(0, \pi)^2$  with exact values given by (46). The domain is partitioned into a family of Voronoi meshes, and for the  $p$ -version the coarsest one employed for the  $h$  version has been used. These results has been obtained using the so called *diagonal* recipe for the stabilization of  $a$  defined as

$$\tilde{S}_a^P(\varphi_i, \varphi_j) = \max(1, a^P(\Pi_k^\nabla \varphi_i, \Pi_k^\nabla \varphi_j))\delta_{ij}$$

where  $\varphi_i$  is the canonical basis in  $V_n(P)$  and  $\delta_{ij}$  is the Kroenecker index, and the following choice for the stabilization of  $b$

$$S_b^P(u_n, v_n) = \frac{h_P}{p^2} \int_{\partial P} u_n v_n ds,$$

which satisfies (29) with  $\beta_*(p) \gtrsim p^{-6}$  and  $\beta^*(p) \lesssim 1$ .

Although these values inserted in the estimates reported in Theorem 12 might seem pessimistic, in reality the numerical results seem to be not affected by the behavior of the stability constants.

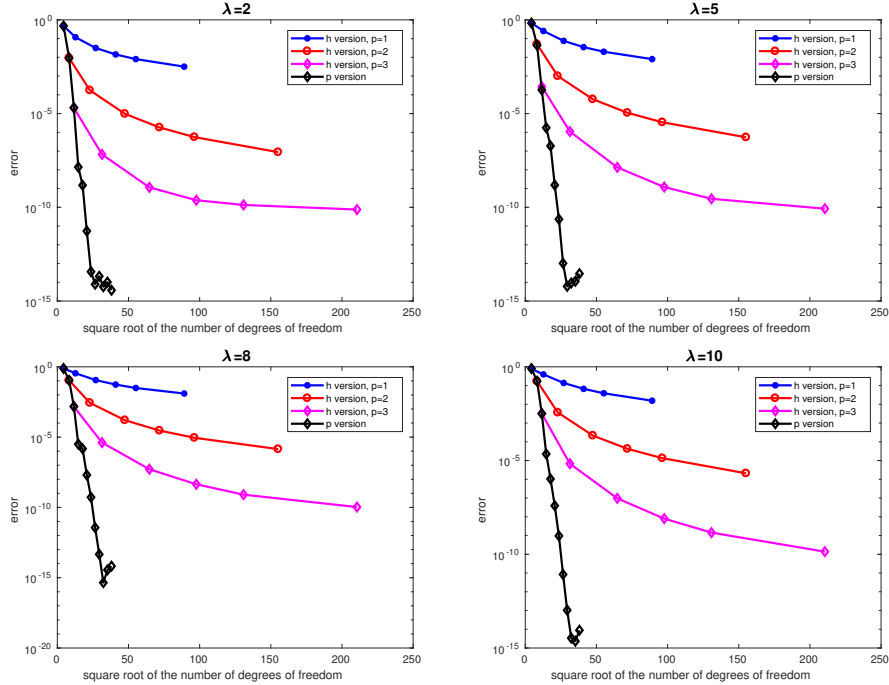


FIGURE 4. Convergence of the error for the first four distinct Dirichlet eigenvalues of the Laplace operator on the unit square domain. On the  $x$ -axis, the square root of the number of degrees of freedom is reported

If the eigenfunctions are not smooth enough, the spectral convergence of  $p$  version of VEM cannot be achieved. However, as in the finite element method, one can resort to the  $hp$  approach which combines the  $p$  and the  $h$  versions using locally

geometrical refined meshes where the solution is singular. For the source problem, the analysis of the exponential convergence of the  $hp$  VEM in presence of corner singularities has been tackled in [7]. The paper [36] merely investigates numerically the convergence of the  $hp$  approximation of the eigenvalues, showing the exponential decay in terms of the cubic root of the number of degrees of freedom, in the case of eigenfunctions with finite Sobolev regularity. We report in Figure 5 the convergence of the error for the first four distinct eigenvalues of the Laplace eigenproblem with Neumann boundary condition on the L-shaped domain obtained in [36]. It is well-known that the first eigenfunction is singular. In order to recover the spectral convergence the  $hp$ -version of VEM has been applied on a graded mesh with a non uniform distribution of  $p$ . The domain has been divided into layers around the reentrant corner and the local polynomial degree of  $V_n(P)$  increases as the layer is farther from the singularity. The results show spectral convergence with respect to the cubic root of the number of degrees of freedom for the  $hp$ -version.

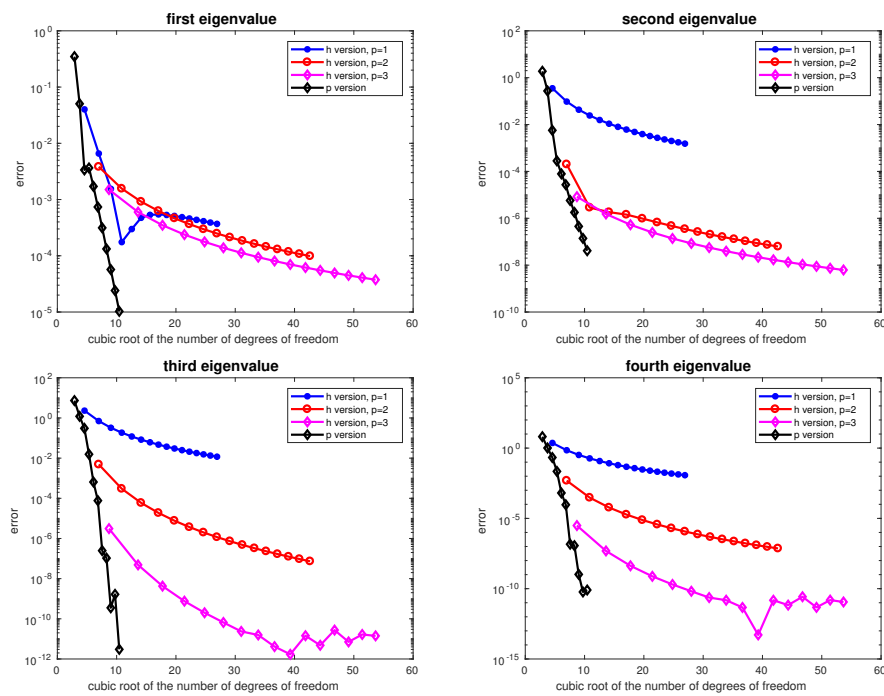


FIGURE 5. Convergence of the error for the first four distinct Neumann eigenvalues of the Laplace operator on the L-shaped domain. Comparison of the  $hp$ -version with the  $h$ -version with  $p = 1, 2, 3$ . On the  $x$ -axis, we report the cubic root of the number of degrees of freedom

## 5. THE CHOICE OF THE STABILIZATION PARAMETERS

In Section 3 we have seen that an effective VEM approximation of eigenvalue problems requires the introduction of appropriate stabilization parameters. In practice, the discrete problem has the form of the following algebraic generalized eigenvalue problem

$$(58) \quad \mathbf{A}\mathbf{u} = \lambda\mathbf{M}\mathbf{u}$$

where both the involved matrices  $\mathbf{A}$  and  $\mathbf{M}$  depend on the stabilization parameters introduced for the VEM discretization.

The results of the previous sections assume that such parameters have been fixed and show the convergence of the method when the meshsize goes to zero and/or  $p$  goes to  $\infty$ . By doing so, it is implicitly understood that the convergence behavior depends on the choice of the parameters. In this section we want to discuss this dependence and see how the discrete solution is influenced by such choice. We would like to make it clear from the very beginning that the optimal strategy for the choice of the parameters is still the object of ongoing research and that the aim of our presentation is more related to the description of the phenomenon than to an ultimate answer to the open questions. Nevertheless, the *easy and quick recipe* will be that the parameter related to  $\mathbf{A}$  should be large enough, while the parameter related to  $\mathbf{M}$  should be small enough and possibly equal to zero.

The results presented in this section are a condensed version of what is published in [13]. The interested reader will find there a more general theory and more specific numerical tests.

Although the general picture of VEM approximation of eigenvalue problems is more complicated, the following simplified setting proves useful in order to understand its main features.

**5.1. A simplified setting.** We assume that all matrices are symmetric and that  $\mathbf{A} = \mathbf{A}_1 + \alpha\mathbf{A}_2$  and  $\mathbf{M} = \mathbf{M}_1 + \beta\mathbf{M}_2$ , where  $\alpha \geq 0$  and  $\beta \geq 0$  play the role of the stabilization parameters. More precisely, we assume that

- i)  $\mathbf{A}_1$  and  $\mathbf{M}_1$  are positive semidefinite;
- ii)  $\mathbf{A}_2$  and  $\mathbf{M}_2$  are positive semidefinite and positive definite on the kernel of  $\mathbf{A}_1$  and  $\mathbf{M}_1$ , respectively;
- iii)  $\mathbf{A}_2$  and  $\mathbf{M}_2$  vanish on the orthogonal complement of the kernel of  $\mathbf{A}_1$  and  $\mathbf{M}_1$ , respectively.

In [13] we have studied several examples and described the spectrum of the generalized eigenvalue problem (58) as a function of  $\alpha$  and  $\beta$ . The main features are easily understood with a simple example when  $\alpha$  or  $\beta$  are constant.

When  $\beta > 0$  is constant, then  $\mathbf{M}$  is positive definite and the eigenvalues of (58) are all positive, possibly vanishing for  $\alpha = 0$  (see assumption i) above), and are formed by two families: the first one is independent on  $\alpha$  and corresponds to eigenvectors  $\mathbf{v}$  orthogonal to the kernel of  $\mathbf{A}_1$  and to the eigenvalues  $\lambda$  that satisfy

$$\mathbf{A}_1\mathbf{v} = \lambda\mathbf{M}\mathbf{v}$$

(see assumption iii) above), while the second family contains eigenvectors  $\mathbf{w}$  in the kernel of  $\mathbf{A}_1$  and the eigenvalues  $\lambda = \alpha\mu$  where  $(\mu, \mathbf{w})$  satisfies

$$\mathbf{A}_2\mathbf{w} = \mu\mathbf{M}\mathbf{w}$$

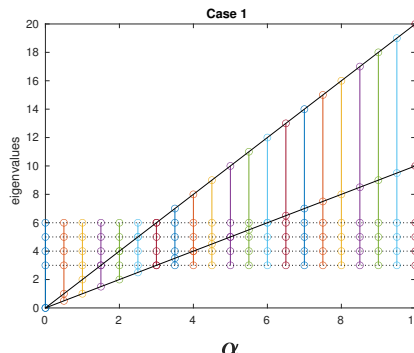


FIGURE 6. Eigenvalues of (58) for  $\beta > 0$  fixed.

(see assumption ii) above). In particular the second family contains eigenvalues growing linearly with  $\alpha$  and includes, for  $\alpha = 0$ , the eigenvalue  $\lambda = 0$  with eigenspace equal to the kernel of  $A_1$ .

Figure 6 gives a graphical indication of the eigenvalues of (58) as a function of  $\alpha$  when  $\beta > 0$  is fixed: the horizontal lines correspond to the eigenvalues of the first family, while the linearly increasing curves starting at the origin correspond to the eigenvalues of the second family.

The second case that is useful to discuss is when  $\alpha > 0$  is fixed and  $\beta$  is varying. This case is analogous to the previous one with the roles of  $A$  and  $M$  exchanged. This means that  $A$  is positive definite and the behavior of the solutions  $(\omega, u)$  to the following eigenvalue problem

$$Mu = \omega Au$$

is analogous to the one depicted in Figure 6 with  $\alpha$  replaced by  $\beta$ . Since the original eigenmodes of problem (58) are given by  $(\lambda, u) = (1/\omega, u)$  for  $\omega \neq 0$  and  $(\infty, u)$  for  $\omega = 0$ , it turns out that the eigenvalues in this case are split again into two families: the first one is independent of  $\beta$  and corresponds to eigenvectors  $v$  orthogonal to the kernel of  $M_1$  and to the eigenvalues  $\lambda = 1/\omega$  that satisfy

$$M_1 v = \omega A v$$

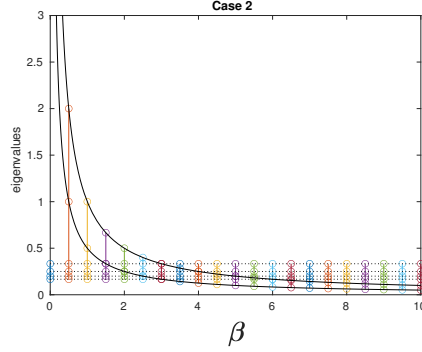
while the second family contains eigenvectors  $w$  in the kernel of  $M_1$  and eigenvalues  $\lambda = 1/(\beta\omega)$  where  $(\omega, w)$  satisfies

$$M_2 w = \omega A w.$$

In particular, the second family contains eigenvalues that behave like decreasing hyperbolas tending to zero as  $\beta$  goes to infinity. For  $\beta = 0$  the eigenvalues of the second family degenerate to  $\lambda = \infty$  with eigenspace equal to the kernel of  $M_1$ .

Figure 7 shows the behavior of the eigensolution of (58) for fixed  $\alpha > 0$  and varying  $\beta$ : the horizontal lines correspond to the eigenvalues of the second family while the hyperbolas represent those of the second one.

**5.2. The role of the VEM stabilization parameters.** The general setting of the problems we have discussed in Section 3 does not fit exactly the simplified framework presented in the previous subsection. In particular, the matrices  $A$  and

FIGURE 7. Eigenvalues of (58) for  $\alpha > 0$  fixed.

$k$	$N = 50$	$N = 100$	$N = 200$	$N = 400$	$N = 800$
Kernel of $A_1$					
1	0	0	0	0	0
2	3	30	99	258	565
3	27	94	246	588	1312
Kernel of $M_1$					
1	0	0	0	0	0
2	0	0	0	0	0
3	0	1	43	182	504

TABLE 2. Dimension of the kernels of  $A_1$  and  $M_1$  with respect to the degree  $k$  and the number of elements  $N$  in the mesh

$M$  do not satisfy the assumptions made above. Nevertheless, a similar splitting into a matrix that is singular due to the presence of the projection operator and a stabilizing matrix that takes care of the kernel of the singular part is present both in  $A$  and  $M$ . Actually, the numerical experiments reveal a dependence on the parameters that resembles pretty much the one presented in Figures 6 and 7.

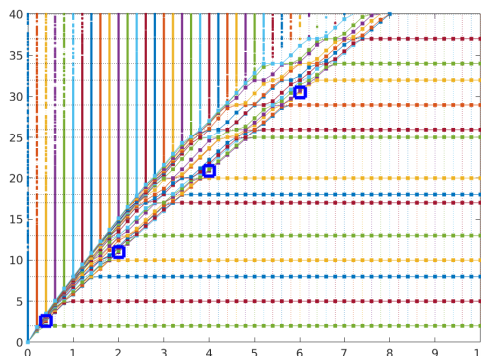
Redirecting the interested reader to [13] for more details, we report here only some results related to the properties of the matrices  $A$  and  $M$ , together with some numerical experiments corresponding to the simplified situations of Figures 6 and 7. All the presented results are taken from [13].

We consider  $\Omega$  as the square of side  $\pi$  and introduce a sequence of five Voronoi meshes of polygons with increasing number of elements from  $N = 50$  to  $N = 800$ . Table 2 reports the dimension of the kernels of the two matrices  $A_1$  and  $M_1$  as a function of the meshsize and of the degree of approximation  $k$ . As it is known, both matrices are non singular in the lowest order case for  $k = 1$ ; the matrix  $M_2$  is non singular for  $k = 2$  as well for the considered meshes.

For completeness, we also computed the lowest eigenvalue of the generalized problem

$$A_1 u = \lambda M_1 u$$

$N = 50$	$N = 100$	$N = 200$	$N = 400$	$N = 800$
1.92654e+00	1.74193e+00	1.06691e+00	6.81927e-01	5.54346e-01

TABLE 3. First eigenvalues of  $\mathbf{A}_1\mathbf{x} = \lambda\mathbf{B}_1\mathbf{x}$  for different meshesFIGURE 8. Eigenvalues computed for  $\beta = 1$  and  $\alpha \in [0, 10]$  with  $k = 3$ 

that is reported in Table 3. The fact that the value of the eigenvalue is decreasing as the number of elements increases, confirms the need for a stabilization.

In the rest of this section we show and comment some results of our computations of the eigenvalues of the Dirichlet problem for the Laplace operator in the case of the mesh  $N = 200$ .

Figure 8 reports the computed eigenvalues in the range  $[0, 40]$ , for  $\beta = 1$  and  $\alpha \in [0, 10]$  with elements of degree  $k = 3$ . Comparing these results with Figure 6 it is easy to recognize the horizontal lines corresponding to the *good* eigenvalues we are interested in. At the same time it is apparent the presence of some oblique lines that correspond to *spurious* modes introduced by the stabilization of  $\mathbf{A}$ .

Figure 9 shows the eigenfunctions corresponding to the marked values of Figure 8 that belong to the same oblique line. It can be seen that the eigenfunctions look similar to each other, which confirms the analogy with the situation presented in Figure 6.

Several other cases when  $\beta \geq 0$  is fixed and  $\alpha$  is varying are reported in Figure 10 for different values of  $k$ .

The last computations of this section involve the situation when  $\alpha > 0$  is fixed and  $\beta$  is varying. Figure 11 shows the behavior of the eigenvalues for different values of  $\alpha$  and  $k$  and with  $\beta$  varying in the interval  $[0, 5]$ ; the analogies with the simplified case shown in Figure 7 are evident.

In conclusion, the reader might wonder what is our suggestion for the choice of the parameters. The answer is not immediate and is not definitive. One clear message is that the dependence on  $\beta$  may have more dangerous effects than the one on  $\alpha$ . As a rule of thumb, our numerical tests indicate that  $\alpha$  should be chosen large enough, possibly using the same criteria adopted for the source problem, while small values of  $\beta$  (or even  $\beta = 0$ ) are preferable. Clearly, a small value of  $\beta$  leads to an ill-conditioned problem: the limit case  $\beta = 0$  may corresponds to a degenerate

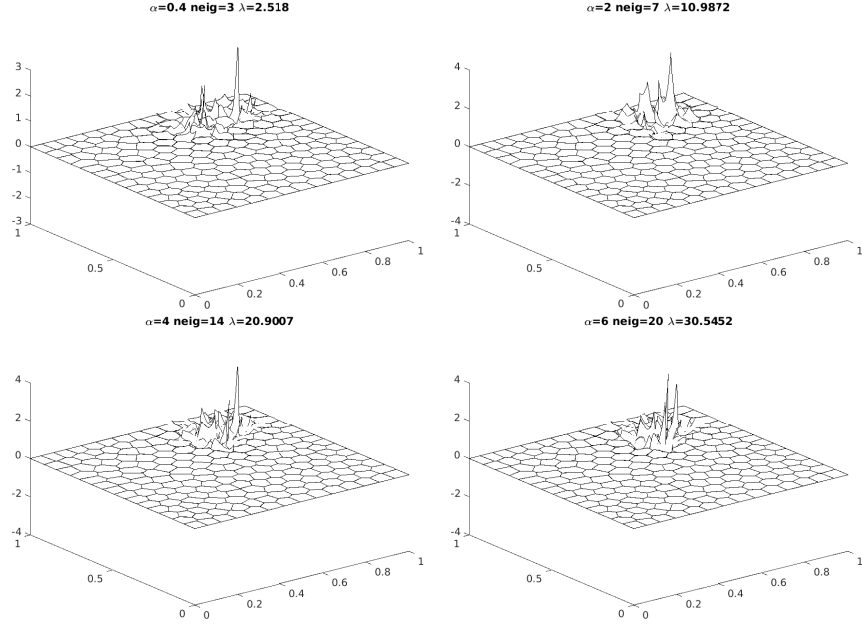


FIGURE 9. Eigenfunctions associated with the marked eigenvalues of Figure 8

eigenvalue problem where the matrix  $M$  is singular. As it is typical for eigenvalue problems, if  $h$  is not small enough the eigenvalues are not yet well resolved and the dependence on the parameters might be more complicated to analyze and may lead to useless results. In order to better illustrate how large values of  $\beta$  can produce wrong results, in Figure 12 we show the computation of the first four eigenvalues with  $\alpha = 10$ ,  $k = 1$ , and  $\beta \in [0, 400]$ . Each subplot represents one of the first four eigenvalues as function of  $\beta$ ; different colors correspond to different meshes. These plots should be compared to Figure 11. In particular, Figure 11(c) shows computations for the same values of  $\alpha$  and  $k$  on the mesh  $N = 200$ . We comment in detail the behavior of the approximation to the fourth eigenvalue shown in the bottom/right subplot of Figure 12; similar considerations apply to the other eigenvalues. First of all, it is clear that if  $h$  is small enough then the solution is correct: when  $N = 6400$  the fourth computed eigenvalue is independent on  $\beta$  and provides a good approximation of  $\lambda = 8$ . On the coarsest mesh, however, the results obtained are useless in order to predict the correct value of the fourth eigenvalue: for large values of  $\beta$  the computed eigenvalue is much smaller than 8 and tends to zero as  $\beta$  increases; for a value of  $\beta$  between 10 and 20 the computed eigenvalue crosses the line  $\lambda = 8$  and it becomes much larger for smaller values of  $\beta$  reaching a value of approximately 12 for  $\beta = 0$ . The results for the next mesh for  $N = 400$  are similar for large  $\beta$  but are significantly different after the red line crosses the value  $\lambda = 8$ . For values of  $\beta$  smaller than the crossing point, the computed eigenvalue remains closer to the correct value of the exact solution. Another interesting phenomenon related to this curve is that when it reaches  $\lambda = 2$  and, more evidently,  $\lambda = 5$ , the curve seems to bend and to be attracted for a



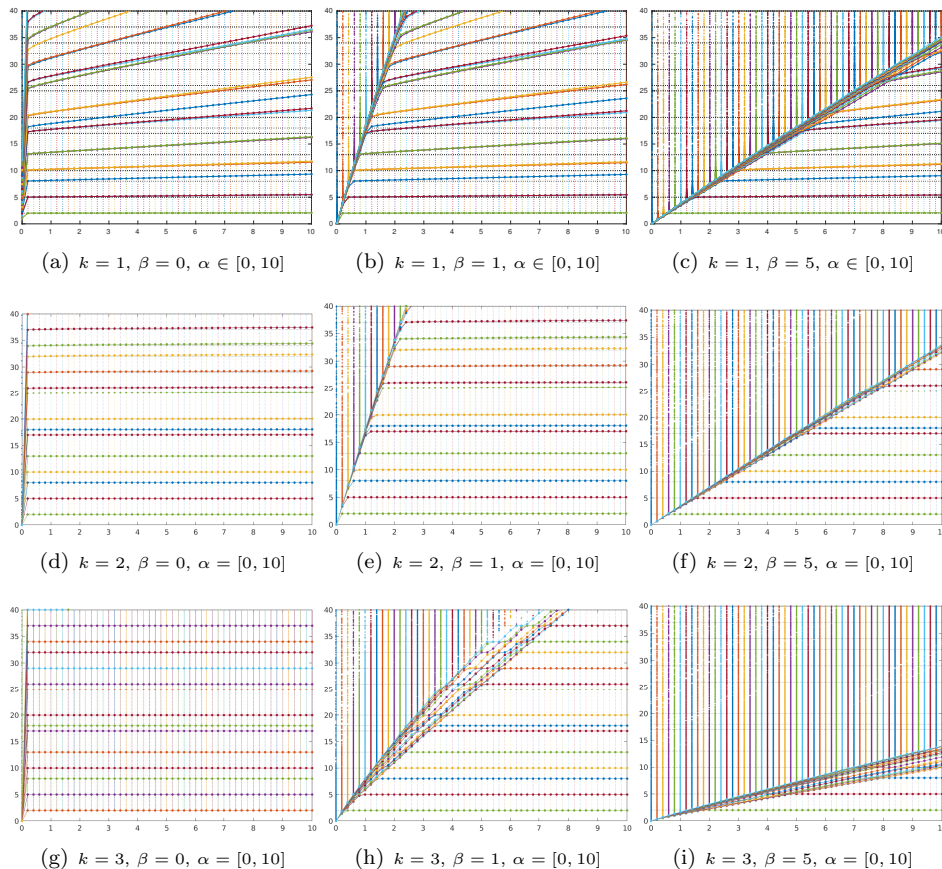


FIGURE 10. Eigenvalues with fixed  $k$  and  $\beta \geq 0$  and varying  $\alpha \in [0, 10]$

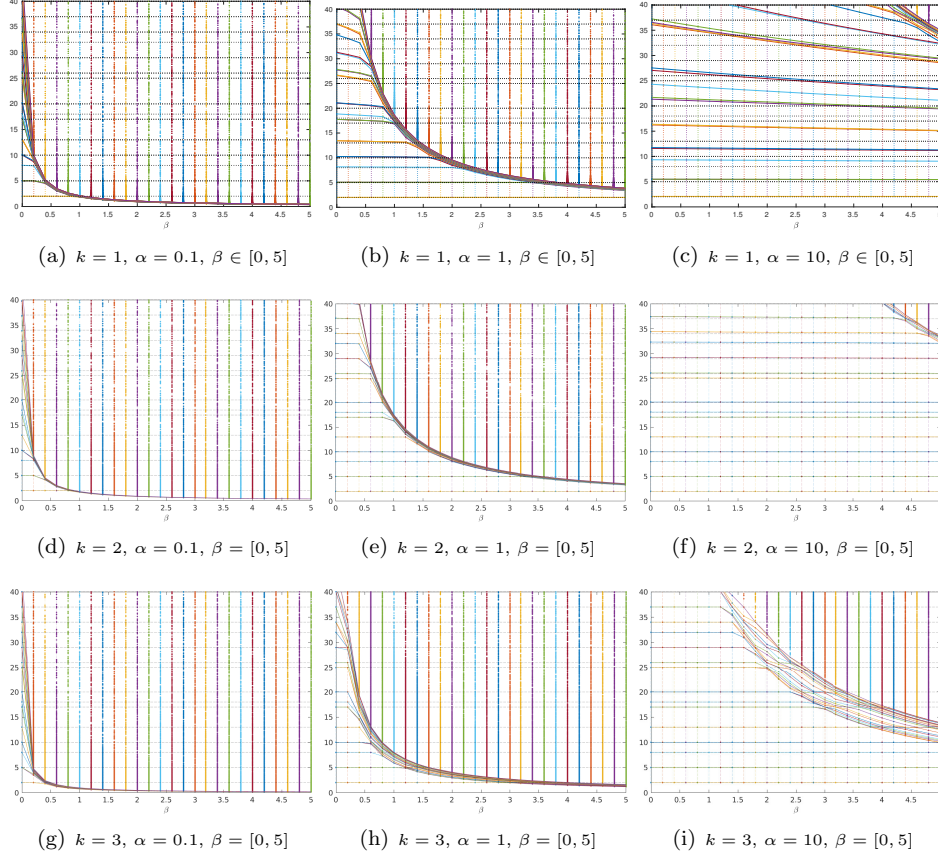
while by the first and second (double) eigenvalue. This behavior is due to the fact that the curve is crossing other computed eigenvalues which are not plotted in this figure and, after the crossing, it continues along another hyperbola.

## 6. APPLICATIONS

We conclude this paper with a discussion on the application of VEM to eigenvalue problems arising from various models and formulations. We start with a presentation of the mixed formulation for our model problem and then we continue with other applications following the chronological order of the related publications.

**6.1. The mixed Laplace eigenvalue problem.** In [29] the mixed formulation of the Laplace eigenvalue is considered. The following usual mixed formulation is considered:  $\Sigma = \mathbf{H}(\text{div}; \Omega)$ ,  $U = L^2(\Omega)$ , so that we are seeking for  $\lambda \in \mathbb{R}$  and a non vanishing  $u \in U$  such that for  $\boldsymbol{\sigma} \in \mathbf{H}(\text{div}; \Omega)$  it holds

$$\begin{aligned} (\boldsymbol{\sigma}, \boldsymbol{\tau}) + (\text{div } \boldsymbol{\tau}, u) &= 0 \quad \forall \boldsymbol{\tau} \in \Sigma \\ (\text{div } \boldsymbol{\sigma}, v) &= -\lambda(u, v) \quad \forall v \in U. \end{aligned}$$

FIGURE 11. Eigenvalues with fixed  $k$  and  $\alpha > 0$  and varying  $\beta \in [0, 5]$ 

It is well known that the analysis of the approximation of the Laplace eigenvalue in mixed form requires particular care because of the lack of compactness of the solution operator with respect to the component  $\sigma$ . The analysis of [29] extends the theory of [11] to the virtual element method. The discrete spaces are constructed as follows: the space  $\Sigma$  is approximated by the following space described in [18]

$$\Sigma_h = \{ \tau_h \in \Sigma : (\tau_h \cdot \mathbf{n})|_e \in \mathbb{P}_k(e) \quad \forall e \in \mathcal{E}_h, \quad \operatorname{div} \tau_h|_P \in \mathbb{P}_{k-1}(P), \\ \operatorname{rot} \tau_h|_P \in \mathbb{P}_{k-1}(P) \quad \forall P \in \mathcal{T}_h \}$$

while the space  $U$  is approximated by a standard piecewise discontinuous space

$$U_h = \{ v_h \in U : v_h|_P \in \mathbb{P}_{k-1}(P) \quad \forall P \in \mathcal{T}_h \}.$$

The matrix form of the approximate problem reads

$$\begin{pmatrix} \mathbf{A} & \mathbf{B}^\top \\ \mathbf{B} & \mathbf{0} \end{pmatrix} \begin{pmatrix} \sigma \\ \mathbf{u} \end{pmatrix} = -\lambda \begin{pmatrix} \mathbf{0} & \mathbf{0} \\ \mathbf{0} & \mathbf{M} \end{pmatrix} \begin{pmatrix} \sigma \\ \mathbf{u} \end{pmatrix}.$$

In this case, the matrix  $\mathbf{M}$  does not contain any stabilization parameter since the space  $U_h$  is a standard mass matrix arising from discontinuous finite elements. The same applies to the matrix  $\mathbf{B}$  that can be constructed directly by using the

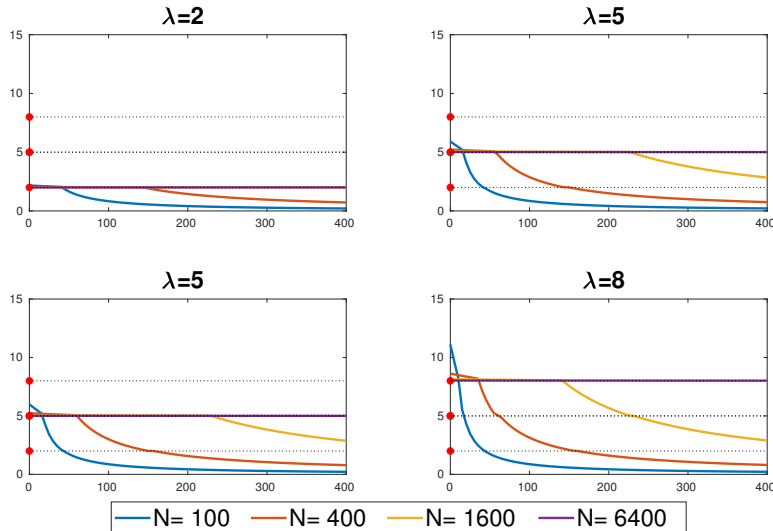


FIGURE 12. First four eigenvalues depending on  $\beta$  for  $\alpha = 10$  and  $k = 1$

degrees of freedom of the spaces  $\Sigma_h$  and  $U_h$ . Hence, the only matrix that requires a stabilization is  $A$ .

The analysis of [29] shows, using the tools of [11] and the properties of the spaces  $\Sigma_h$  and  $U_h$ , the following uniform bound for the solution of the source problem with right hand side  $f \in L^2(\Omega)$ :

$$\|\sigma - \sigma_h\|_0 + \|u - u_h\|_0 \leq Ch^t \|f\|_0$$

where  $t = \min(k, r)$ ,  $r$  being such that  $u \in H^{1+r}(\Omega)$  (see (13)). From this estimate the convergence of the eigenvalues and eigenfunctions follows by standard arguments and an appropriate definition of the solution operator (see Section 2 and [10]).

**6.2. The Steklov eigenvalue problem.** Another formulation where the stabilization parameter enters only the matrix on the left hand side of the discrete system, is given by the so called Steklov eigenvalue problem

$$\begin{aligned} \Delta u &= 0 & \text{in } \Omega \\ \frac{\partial u}{\partial \mathbf{n}} &= \lambda u & \text{on } \partial\Omega. \end{aligned}$$

A more general setting could be actually considered by taking the second equation only on a subset  $\Gamma_0$  of  $\partial\Omega$  and homogeneous Neumann boundary conditions on the remaining part of the boundary. We refer to [31] for the analysis of its VEM discretization.

The variational formulation is obtained by considering  $V = H^1(\Omega)$  and seeks for  $\lambda \in \mathbb{R}$  and a non vanishing  $u \in V$  such that

$$\int_{\Omega} \nabla u \cdot \nabla v \, dx = \lambda \int_{\partial\Omega} uv \, ds \quad \forall v \in V.$$

Since the bilinear form on the left hand side is not  $H^1(\Omega)$ -elliptic, the analysis is based on the use of a shift argument by adding the boundary integral on both sides of the eigenvalue problem in weak form. Hence, the resolvent operator and its discrete counterpart are defined using the shifted problem. In this case, it is necessary to consider  $T : V \rightarrow V$  in order to give sense to the datum of the source problem.

The approximation of the problem makes use of the standard VEM spaces described in Section 3. As we have seen before, the discrete problem requires to introduce a discretization of the bilinear form on the left hand side, with the addition of a stabilization term. Whereas, the integral on the right hand side can be computed using the degrees of freedom on the element boundaries.

For  $f \in H^1(\Omega)$ , the solution to the associated source problem belongs to  $H^{1+r}(\Omega)$ , with  $r > \frac{1}{2}$ . This implies that the resolvent operator is compact on  $V$ , so that the analysis in [31] relies on the standard theory for compact operators that we have recalled in Section 2. In particular, it is based on the following uniform convergence of  $T_h$  to  $T$ :

$$\|(T - T_h)f\|_1 \leq Ch^r \|f\|_1 \quad \forall f \in H^1(\Omega),$$

which in turn gives the same rate of convergence for the gap between eigenspaces and double rate of convergence for the eigenvalue error.

The matrix form of the discrete problem is

$$Au = \lambda Mu,$$

where  $A$  depends on the stabilization parameter  $\alpha_P$ . In [31] one can find an interesting test case which models the sloshing modes of a two dimensional fluid contained in a square. In this test case,  $\Omega$  is the unit square and its boundary is divided into two parts:  $\Gamma_0$  the top side of the square and  $\Gamma_1$  the remaining three sides. On  $\Gamma_0$  the Steklov condition is imposed, while on  $\Gamma_1$  homogeneous Neumann condition is enforced. The convergence analysis with fixed parameter  $\alpha_P = 1$  for all  $P \in \mathcal{T}_h$  confirms the theoretical results. The paper contains, for the first time, the study of the effect of the stability on the computed eigenvalues on a fixed mesh. It has been observed that, when  $\alpha_P$  is independent of the element  $P$  and varies from  $4^{-3}$  to  $4^3$  spurious eigenvalues appear among the correct ones. In Figure 13, we plot the first 16 eigenvalues reported in [31, Table 3]. These eigenvalues were been obtained using a triangular mesh, considering the middle point of each edge as a new vertex of the polygon. Each side of the square has been divided into 8 parts and virtual elements with  $k = 1$  are applied. The plot on the right is a zoom of the one on the left. The dotted black horizontal lines represent the first 3 exact eigenvalues. One can see that for  $\alpha_P > 1$  the spurious eigenvalues seems to be proportional to the stabilization parameter and this appears to be in agreement with the analysis reported in Section 5, while the approximation of the three correct ones is independent of  $\alpha_P$ .

**6.3. An acoustic vibration problem.** The next application has been considered in [8] and is an example where only the matrix on the right hand side of the discrete algebraic system contains a parameter.

The model describes the free vibrations of an inviscid compressible fluid within a bounded rigid cavity  $\Omega$ . The simplest model consists in finding eigenvalues  $\lambda \in \mathbb{R}$

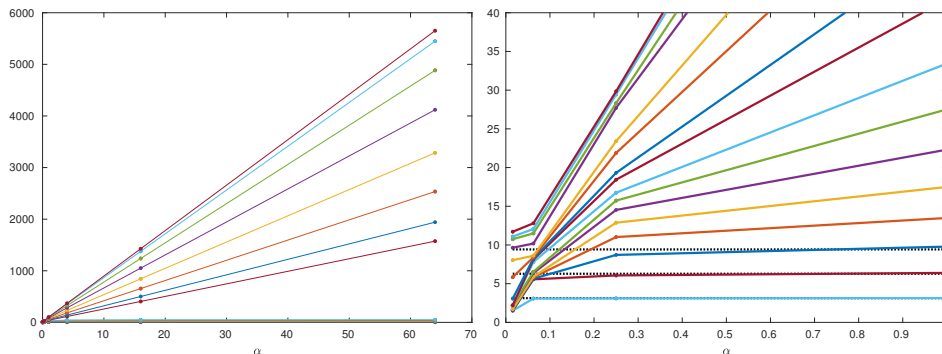


FIGURE 13. First 16 eigenvalues for  $4^{-3} \leq \alpha_P \leq 4^3$

and non vanishing eigenfunctions  $\mathbf{u} \in \mathbf{H}_0(\text{div}; \Omega)$  such that

$$\int_{\Omega} \text{div } \mathbf{u} \text{ div } \mathbf{v} \, dx = \lambda \int_{\Omega} \mathbf{u} \cdot \mathbf{v} \, dx \quad \forall \mathbf{v} \in \mathbf{H}_0(\text{div}; \Omega).$$

Here  $\mathbf{H}_0(\text{div}; \Omega)$  is the subspace of  $\mathbf{H}(\text{div}; \Omega)$  of functions with vanishing trace of the normal component on  $\partial\Omega$ .

The approximation is performed by the following VEM space that has been designed taking inspiration from [6, 18]:

$$V_h = \{ \mathbf{v}_h \in \mathbf{H}_0(\text{div}; \Omega) : (\mathbf{v}_h \cdot \mathbf{n})|_e \in \mathbb{P}_k(e) \, \forall e \in \mathcal{E}_h, \text{div } \mathbf{v}_h|_P \in \mathbb{P}_k(P), \\ \text{rot } \mathbf{v}_h|_P = 0 \, \forall P \in \mathcal{T}_h \}.$$

The discretized problem has the classical form

$$\mathbf{A}u = \lambda \mathbf{M}u$$

and the matrix  $\mathbf{A}$  can be formed directly using the degrees of freedom since the divergence of elements in  $V_h$  are piecewise polynomials. On the other hand, the mass matrix  $\mathbf{M}$  should be constructed by using the typical VEM approach and requires a stabilization in order to control the non polynomial part of the space  $V_h$ .

The convergence analysis of [8] is performed as in case of standard finite elements [9] by shifting the solution operator in order to deal with the kernel of the divergence operator, and by exploiting the theory of [23] related to the analysis of non compact operators. More precisely, the continuous solution operator  $T : \mathbf{H}_0(\text{div}; \Omega) \rightarrow \mathbf{H}_0(\text{div}; \Omega)$  is defined as the solution  $T\mathbf{f} \in \mathbf{H}_0(\text{div}; \Omega)$  of

$$\int_{\Omega} \text{div } T\mathbf{f} \text{ div } \mathbf{v} \, dx + \int_{\Omega} T\mathbf{f} \cdot \mathbf{v} \, dx = \int_{\Omega} \mathbf{f} \cdot \mathbf{v} \, dx \quad \forall \mathbf{v} \in \mathbf{H}_0(\text{div}; \Omega)$$

and its discrete counterpart  $T_h : V_h \rightarrow V_h$  is defined as the solution  $T_h\mathbf{f}_h \in V_h$  of

$$\int_{\Omega} \text{div } T_h\mathbf{f}_h \text{ div } \mathbf{v}_h \, dx + \int_{\Omega} T_h\mathbf{f}_h \cdot \mathbf{v}_h \, dx = \int_{\Omega} \mathbf{f}_h \cdot \mathbf{v}_h \, dx \quad \forall \mathbf{v}_h \in V_h.$$

The theory of [23] consists in showing the following mesh dependent uniform convergence

$$\lim_{h \rightarrow 0} \sup_{\substack{\mathbf{f}_h \in V_h \\ \|\mathbf{f}_h\|_{\text{div}}=1}} \|(T - T_h)\mathbf{f}_h\|_{\text{div}} = 0$$

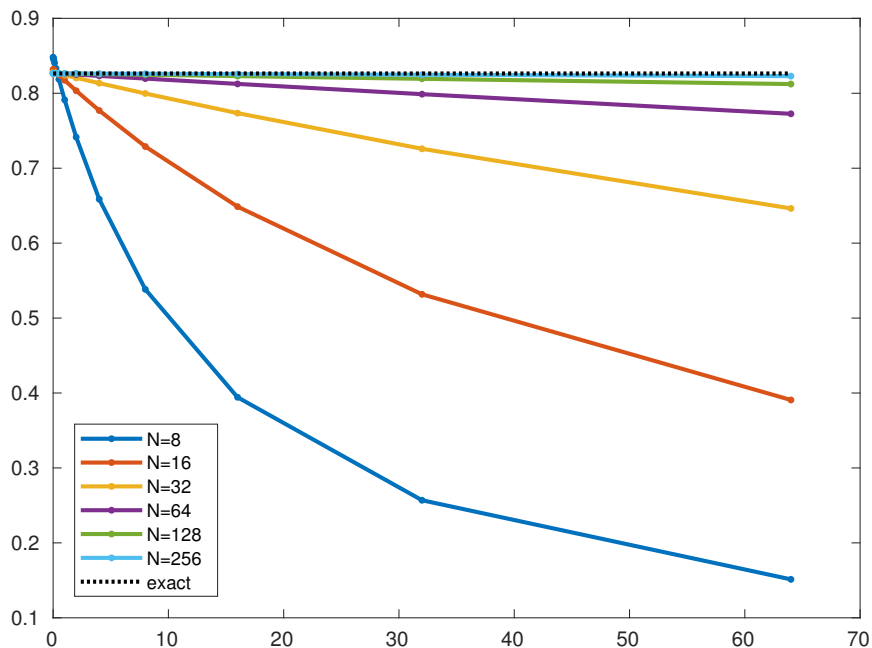


FIGURE 14. First eigenvalue with  $2^{-6} \leq \beta \leq 2^6$  and different meshes

together with the density of  $V_h$  in  $\mathbf{H}_0(\text{div}; \Omega)$ . In particular, in [8] it is proved the following estimate

$$\sup_{\substack{\mathbf{f}_h \in V_h \\ \|\mathbf{f}_h\|_{\text{div}}=1}} \|(T - T_h)\mathbf{f}_h\|_{\text{div}} \leq Ch^s,$$

where  $s \in [\frac{1}{2}, 1]$  is the regularity index of the solution to the associated source problem. This result implies that for  $h$  small enough the virtual element method does not introduce spurious eigenvalues interspersed among the physical ones we are interested in. Optimal error estimates depending on the regularity of the eigenfunctions follow by combining the technique of [24] with the first Strang lemma.

The above theoretical results were obtained when the stability parameter  $\beta_P$  is positive. The numerical experiments show that for  $k = 0$  the optimal second order rate of convergence for the eigenvalues can be achieved for several choices of meshes. The effect of the stability constant has also been investigated. In Figure 14, we plot the first eigenvalue for  $\beta_P$  ranging from  $2^{-6}$  to  $2^6$  for different square meshes as reported in [8, Table 4]. It can be seen that as the mesh gets finer the results are less sensible to the value of  $\beta_P$ , while for coarse meshes the behavior looks similar to that shown in Figure 12 corresponding to Case 2 in Section 5. Moreover, although the choice  $\beta_P = 0$  is not covered by the theory, the computational results appear to be very accurate in this case, and also this is in agreement with the observations reported in Section 5.

**6.4. Eigenvalue problems related to plate models.** The computation of vibration frequencies and modes of an elastic solid is a very important topic in engineering applications. This and the following sections are devoted to report on

the results obtained in [32, 34, 30] concerning the use of VEM to approximate the eigenvalues of the Kirchhoff–Love model for plates and of linear elasticity equations.

We consider a plate whose mean surface, in its reference configuration, occupies a polygonal bounded domain  $\Omega \subset \mathbb{R}^2$ . The plate is clamped on its whole boundary. Let  $u$  denote the transverse displacement and  $\lambda$  the vibration frequency, then the plate vibration problem, modeled by Kirchhoff–Love equations reads: find  $\lambda \in \mathbb{R}$  and a non vanishing  $u$  such that:

$$\begin{aligned} \Delta^2 u &= \lambda u & \text{in } \Omega \\ u &= \frac{\partial u}{\partial \mathbf{n}} = 0 & \text{on } \partial\Omega. \end{aligned}$$

The corresponding weak form reads: find  $(\lambda, u) \in \mathbb{R} \times H_0^2(\Omega)$  with  $u \neq 0$  such that

$$(59) \quad \int_{\Omega} D^2 u : D^2 v \, dx = \lambda \int_{\Omega} uv \, dx \quad \forall v \in H_0^2(\Omega),$$

where  $D^2 v$  denotes the Hessian matrix of  $v$ . The associated resolvent operator  $T$  is defined for all  $f \in H_0^2(\Omega)$  as the solution  $Tf$  of the corresponding source problem. It results to be self adjoint and compact thanks to the fact that  $Tf$  belongs to  $H^{2+s}(\Omega)$  for some  $s \in ]\frac{1}{2}, 1]$  being the Sobolev regularity for the biharmonic equation with homogeneous Dirichlet boundary conditions.

We recall here the construction of the virtual elements space proposed in [32] which differs from those presented in the previous sections since  $C^1$ -regularity is required for approximating functions in  $H_0^2(\Omega)$ . Given a sequence  $\{\mathcal{T}_h\}_h$  of decompositions of  $\Omega$  into polygons  $P$ , we introduce first the following finite dimensional space:

$$\begin{aligned} V_h(P) &= \left\{ v_h \in H^2(P) : \Delta^2 v_h \in \mathbb{P}_2(P), v_h|_{\partial P} \in C^0(\partial P), \right. \\ &\quad \left. \nabla v_h|_{\partial P} \in C^0(\partial P)^2, v_h|_e \in \mathbb{P}_3(e), \frac{\partial v_h}{\partial \mathbf{n}} \Big|_e \in \mathbb{P}_1(e) \forall e \in \partial P \right\}. \end{aligned}$$

The corresponding degrees of freedom are the values of  $v_h$  and  $\nabla v_h$  at the vertices of  $P$ . Using these degrees of freedom it is possible to define a projection operator  $\Pi_2^\Delta : V_h(P) \rightarrow \mathbb{P}_2(P) \subseteq V_h(P)$  by solving for each  $v \in V_h(P)$  the following problem:

$$\begin{aligned} a_\Delta^P(\Pi_2^\Delta v, q) &= a_\Delta^P(v, q) & \forall q \in \mathbb{P}_2(P) \\ ((\Pi_2^\Delta v, q))_P &= ((v, q))_P & \forall q \in \mathbb{P}_1(P), \end{aligned}$$

where

$$a_\Delta^P(u, v) = \int_P D^2 u : D^2 v \, dx, \quad ((v, q))_P = \sum_{i=1}^{N_P} u(V_i) v(V_i) \quad \forall u, v \in H^2(P),$$

and  $V_i$   $i = 1, \dots, N_P$  are the vertices of  $P$ .

Then the local virtual space is:

$$W_h(P) = \left\{ v_h \in V_h(P) : \int_P (\Pi_2^\Delta v_h - v_k) q \, dx = 0 \forall q \in \mathbb{P}_2(P) \right\}.$$

Thanks to this characterization of  $W_h(P)$ , the  $L^2(P)$ -projection operator onto  $\mathbb{P}_2(P)$  coincides with  $\Pi_2^\Delta$ .

With the above definitions, the global virtual space is defined as:

$$W_h = \{v_h \in H_0^2(\Omega) : v_h|_P \in W_h(P)\}$$

and the discrete bilinear forms are given for all  $u_h, v_h \in W_h$  by

$$a_h(u_h, v_h) = \sum_{P \in \mathcal{T}_h} a_{\Delta, h}^P(u_h, v_h), \quad b_h(u_h, v_h) = \sum_{P \in \mathcal{T}_h} b_{\Delta, h}^P(u_h, v_h),$$

with

$$\begin{aligned} a_{\Delta, h}^P(u_h, v_h) &= a_{\Delta}^P(\Pi_2^\Delta u_h, \Pi_2^\Delta v_h) + s_{\Delta, a}^P(u_h - \Pi_2^\Delta u_h, v_h - \Pi_2^\Delta v_h) \\ b_{\Delta, h}^P(u_h, v_h) &= \int_P \Pi_2^\Delta u_h \Pi_2^\Delta v_h \, dx + s_{\Delta, b}^P(u_h - \Pi_2^\Delta u_h, v_h - \Pi_2^\Delta v_h). \end{aligned}$$

As usual the stabilization terms  $s_{\Delta, a}^P$  and  $s_{\Delta, b}^P$  have been added in order to guarantee consistency and stability.

With the above definitions, the discrete counterpart of equation (59) reads: find  $(\lambda_h, u_h) \in \mathbb{R} \times W_h$  with  $u \neq 0$  such that

$$a_h(u_h, v_h) = \lambda_h b_h(u_h, v_h) \quad \forall v_h \in W_h.$$

After introducing the resolvent operator  $T_h : W_h \rightarrow W_h$  as the mapping that associates to any  $f_h \in W_h$  the solution  $T_h f_h$  to the corresponding source problem, the convergence analysis follows from the theory developed in [23, 24] and gives optimal rate of convergence for the gap between continuous and discrete eigenspaces according to the regularity of the eigenfunctions and double rate of convergence for the eigenvalue error.

The numerical results require that the choice for the stabilization terms is made precise, therefore using the degrees of freedom of the local space one can set

$$\begin{aligned} s_{\Delta, a}^P(u_h, v_h) &= \alpha_P \sum_{i=1}^{N_P} (u_h(V_i) v_h(V_i) + h_{V_i}^2 \nabla u_h(V_i) \cdot \nabla v_h(V_i)) \\ s_{\Delta, b}^P(u_h, v_h) &= \beta_P \sum_{i=1}^{N_P} (u_h(V_i) v_h(V_i) + h_{V_i}^2 \nabla u_h(V_i) \cdot \nabla v_h(V_i)) \end{aligned}$$

for all  $u_h, v_h \in W_h(P)$ . In the numerical experiments presented in [32], the stabilization parameters  $\alpha_P$  and  $\beta_P$  are chosen as the mean value of the eigenvalues of the local matrices  $a_{\Delta}^P(\Pi_2^\Delta u_h, \Pi_2^\Delta v_h)$  and  $\int_P \Pi_2^\Delta u_h \Pi_2^\Delta v_h \, dx$ , respectively. Hence, the matrices  $A$  and  $M$  of the associated algebraic eigenvalue problem  $Au = \lambda Mu$  depend on stabilization parameters and we shall discuss later on their choice.

The numerical results reported in [32] show that the first four eigenvalues converge to the exact or extrapolated values with quadratic rate in agreement with the theoretical results.

In order to analyze the effect of the parameters on the computed eigenvalues, in [32] it has been done the choice to multiply the stabilizing forms  $s_{\Delta, a}^P$  and  $s_{\Delta, b}^P$  by the same value of the parameter. This makes very difficult to compare the results with the behavior described in Section 5, since the better choice would be to take large values of  $\alpha_P$  and small ones of  $\beta_P$ . Coherently, the conclusions of [32] is that the optimal choice is for value of the parameter in the middle.

We end this subsection with some consideration relative to the buckling problem of a clamped plate, which can be formulated as a spectral problem of fourth order as follows: given a plane stress tensor field  $\boldsymbol{\eta} : \Omega \rightarrow \mathbb{R}^{2 \times 2}$ , find the non vanishing



deflection of the plate  $u$  and the eigenvalue (the buckling coefficient)  $\lambda$  such that

$$\begin{aligned} \Delta^2 u &= -\lambda \operatorname{div}(\boldsymbol{\eta} \nabla u) && \text{in } \Omega \\ u &= \frac{\partial u}{\partial \mathbf{n}} = 0 && \text{on } \partial\Omega. \end{aligned}$$

Setting  $a_\Delta(u, v) = \int_\Omega D^2 u : D^2 v \, dx$  and  $b_b(u, v) = \int_\Omega \boldsymbol{\eta} \nabla u \nabla v \, dx$  the weak problem can be written as (59) with  $b_b(u, v)$  on the right hand side instead of the  $L^2(\Omega)$ -scalar product.

The virtual element discretization of this problem has been discussed in [34] using virtual element spaces of any degree  $k \geq 2$  introduced in [19]:

$$V_h(P) = \left\{ v_h \in \tilde{V}_h(P) : \int_P (v_h - \Pi_k^\Delta v_h) q \, dx = 0 \, \forall q \in \mathbb{P}_{k-3}^*(P) \cup \mathbb{P}_{k-2}^*(P) \right\}$$

where  $\mathbb{P}_\ell^*(P)$  denotes homogeneous polynomials of degree  $\ell$  with the convention that  $\mathbb{P}_{-1}^*(P) = \{0\}$ . In the definition above the following notation have been used: for  $r = \max(3, k)$  and  $s = k - 1$

$$\begin{aligned} \tilde{V}_h(P) &= \left\{ v_h \in H^2(P) : \Delta^2 v_h \in \mathbb{P}_{k-2}(P), v_h|_{\partial P} \in C^0(\partial P), \right. \\ &\quad \left. \nabla v_h|_{\partial P} \in C^0(\partial P)^2, v_h|_e \in \mathbb{P}_r(e), \frac{\partial v_h}{\partial \mathbf{n}} \Big|_e \in \mathbb{P}_s(e) \, \forall e \in \partial P \right\}. \end{aligned}$$

and  $\Pi_k^\Delta : H^2(P) \rightarrow \mathbb{P}_k(P) \subseteq \tilde{V}_h(P)$  is the computable projection operator solution of local problems:

$$\begin{aligned} a_\Delta^P(\Pi_k^\Delta v, q) &= a_\Delta^P(v, q) \quad \forall q \in \mathbb{P}_k(P) \quad \forall v \in H^2(P) \\ \widehat{\Pi_k^\Delta v} &= \widehat{v}, \quad \widehat{\nabla \Pi_k^\Delta v} = \widehat{\nabla v} \end{aligned}$$

with  $\widehat{v} = \frac{1}{N_P} \sum_{i=1}^{N_P} v(V_i)$ , and  $V_i$  the  $N_P$  vertices of  $P$ . Then the discrete bilinear form  $a_h$  is the sum of local terms composed by a consistency and a stabilizing part

$$a_h^P(u_h, v_h) = a_\Delta^P(\Pi_k^\Delta u_h, \Pi_k^\Delta v_h) + s_{\Delta, a}^P(u_h - \Pi_k^\Delta u_h, v_h - \Pi_k^\Delta v_h).$$

On the other hand the discrete right hand side can be constructed using the degrees of freedom without the necessity of stabilizing

$$b_b^P(u_h, v_h) = \int_P \boldsymbol{\eta} \Pi_{k-1}^\Delta u_h \Pi_{k-1}^\Delta v_h \, dx.$$

The analysis of this problem follows the same lines as the one for the vibrating plate reported above. In [34] the theoretical results are confirmed by several numerical experiments showing that the method produces accurate solutions.

Another eigenvalue problem that involves a fourth order operator and whose approximation has been analyzed when VEM spaces are used, can be found in [33] where a transmission problem is considered.

**6.5. Eigenvalue problems related to linear elasticity models.** In this section we report on the analysis presented in [30] about the VEM approximation of the linear elasticity eigenvalue problem in two space dimensions. We consider the functional space  $V = H_{\Gamma_D}^1(\Omega)^2$ , where  $\Gamma_D$  is the part of  $\partial\Omega$  where homogeneous Dirichlet boundary condition are imposed, that is where the displacement of the

structure is prescribed and equal to zero. The equation we are interested in is: find  $\lambda \in \mathbb{R}$  and  $\mathbf{u} \in V$  different from zero such that

$$\int_{\Omega} \mathcal{C} \underline{\varepsilon}(\mathbf{u}) : \underline{\varepsilon}(\mathbf{v}) \, d\mathbf{x} = \lambda \int_{\Omega} \rho \mathbf{u} \cdot \mathbf{v} \, d\mathbf{x},$$

where  $\rho > 0$  is the density of the material,  $\underline{\varepsilon}$  is the symmetric gradient, and the compliance tensor  $\mathcal{C}$  is defined as

$$\mathcal{C}\boldsymbol{\tau} = 2\mu\boldsymbol{\tau} + \lambda\text{tr}(\boldsymbol{\tau})\mathbf{I},$$

$\mu$  and  $\lambda$  being the Lamé constants.

It is well known that the problem under consideration is associated with a compact resolvent operator, so that the analysis of its approximation relies on the standard Babuška–Osborn theory.

The VEM discretization makes use of the natural vectorial generalization  $V_h \subset V$  based on the local standard spaces (14) and of the projection operator defined as in (15) with the due modifications.

The discrete problem has the standard form of a generalized eigenvalue problem  $\mathbf{A}\mathbf{u} = \lambda\mathbf{M}\mathbf{u}$ , where both matrices  $\mathbf{A}$  and  $\mathbf{M}$  contain a stabilization parameter. The analysis, both a priori and a posteriori, is performed for a given choice of the stabilizing parameters, which is analogous to the one described in Section 3.4 As in [32], see also Section 6.4, in [30] a study on the dependence of the stabilizing parameters is performed when the parameters of  $\mathbf{A}$  and  $\mathbf{M}$  are chosen equal to each other. It turns out that when the parameter is not too large or not too small, the first eigenvalues of the considered example are not polluted by spurious modes. This is compatible with what we have found in Section 5, although a safer choice would imply to take a larger parameter for stabilizing the matrix  $\mathbf{A}$  and a smaller one (or even zero) for  $\mathbf{M}$ .

## REFERENCES

- [1] S. Agmon. *Lectures on elliptic boundary value problems*. Prepared for publication by B. Frank Jones, Jr. with the assistance of George W. Batten, Jr. Van Nostrand Mathematical Studies, No. 2. D. Van Nostrand Co., Inc., Princeton, N.J.-Toronto-London, 1965.
- [2] B. Ahmad, A. Alsaedi, F. Brezzi, L. D. Marini, and A. Russo. Equivalent projectors for virtual element methods. *Comput. Math. Appl.*, 66(3):376–391, 2013.
- [3] B. Ayuso de Dios, K. Lipnikov, and G. Manzini. The nonconforming virtual element method. *ESAIM Math. Model. Numer. Anal.*, 50(3):879–904, 2016.
- [4] I. Babuška and J. Osborn. Eigenvalue problems. In *Handbook of numerical analysis, Vol. II*, Handb. Numer. Anal., II, pages 641–787. North-Holland, Amsterdam, 1991.
- [5] L. Beirão da Veiga, F. Brezzi, A. Cangiani, G. Manzini, L. D. Marini, and A. Russo. Basic principles of virtual element methods. *Math. Models Methods Appl. Sci.*, 23(1):199–214, 2013.
- [6] L. Beirão da Veiga, F. Brezzi, L. D. Marini, and A. Russo. Mixed virtual element methods for general second order elliptic problems on polygonal meshes. *ESAIM Math. Model. Numer. Anal.*, 50(3):727–747, 2016.
- [7] L. Beirão da Veiga, A. Chernov, L. Mascotto, and A. Russo. Basic principles of  $hp$  virtual elements on quasiuniform meshes. *Math. Models Methods Appl. Sci.*, 26(8):1567–1598, 2016.
- [8] L. Beirão da Veiga, D. Mora, G. Rivera, and R. Rodríguez. A virtual element method for the acoustic vibration problem. *Numer. Math.*, 136(3):725–763, 2017.
- [9] A. Bermúdez, R. Durán, M. A. Muschietti, R. Rodríguez, and J. Solomin. Finite element vibration analysis of fluid-solid systems without spurious modes. *SIAM J. Numer. Anal.*, 32(4):1280–1295, 1995.
- [10] D. Boffi. Finite element approximation of eigenvalue problems. *Acta Numer.*, 19:1–120, 2010.

- [11] D. Boffi, F. Brezzi, and L. Gastaldi. On the convergence of eigenvalues for mixed formulations. *Ann. Scuola Norm. Sup. Pisa Cl. Sci. (4)*, 25(1-2):131–154 (1998), 1997. Dedicated to Ennio De Giorgi.
- [12] D. Boffi, F. Brezzi, and L. Gastaldi. On the problem of spurious eigenvalues in the approximation of linear elliptic problems in mixed form. *Math. Comp.*, 69(229):121–140, 2000.
- [13] D. Boffi, F. Gardini, and L. Gastaldi. Approximation of PDE eigenvalue problems involving parameter dependent matrices. *Calcolo*, 57(4):41, 2020.
- [14] Daniele Boffi, Annalisa Buffa, and Lucia Gastaldi. Convergence analysis for hyperbolic evolution problems in mixed form. *Numer. Linear Algebra Appl.*, 20(4):541–556, 2013.
- [15] Daniele Boffi and Lucia Gastaldi. Analysis of finite element approximation of evolution problems in mixed form. *SIAM J. Numer. Anal.*, 42(4):1502–1526, 2004.
- [16] S. C. Brenner. Poincaré-Friedrichs inequalities for piecewise  $H^1$  functions. *SIAM J. Numer. Anal.*, 41(1):306–324, 2003.
- [17] S. C. Brenner and L. R. Scott. *The mathematical theory of finite element methods*, volume 15 of *Texts in Applied Mathematics*. Springer, New York, third edition, 2008.
- [18] F. Brezzi, R. S. Falk, and L. D. Marini. Basic principles of mixed virtual element methods. *ESAIM Math. Model. Numer. Anal.*, 48(4):1227–1240, 2014.
- [19] F. Brezzi and L. D. Marini. Virtual element methods for plate bending problems. *Comput. Methods Appl. Mech. Engrg.*, 253:455–462, 2013.
- [20] A. Cangiani, E. H. Georgoulis, T. Pryer, and O. J. Sutton. A posteriori error estimates for the virtual element method. *Numer. Math.*, 137(4):857–893, 2017.
- [21] P. G. Ciarlet. *The finite element method for elliptic problems*. North-Holland Publishing Co., Amsterdam-New York-Oxford, 1978. Studies in Mathematics and its Applications, Vol. 4.
- [22] M. Dauge. Benchmark computations for maxwell equations for the approximation of highly singular solutions. URL <http://perso.univ-rennes1.fr/monique.dauge/benchmark.html>, 2004.
- [23] J. Descloux, N. Nassif, and J. Rappaz. On spectral approximation. I. The problem of convergence. *RAIRO Anal. Numér.*, 12(2):97–112, iii, 1978.
- [24] J. Descloux, N. Nassif, and J. Rappaz. On spectral approximation. II. Error estimates for the Galerkin method. *RAIRO Anal. Numér.*, 12(2):113–119, iii, 1978.
- [25] F. Gardini, G. Manzini, and G. Vacca. The nonconforming virtual element method for eigenvalue problems. *ESAIM Math. Model. Numer. Anal.*, 53(3):749–774, 2019.
- [26] F. Gardini and G. Vacca. Virtual element method for second-order elliptic eigenvalue problems. *IMA J. Numer. Anal.*, 38(4):2026–2054, 2018.
- [27] P. Grisvard. *Elliptic problems in nonsmooth domains*, volume 69 of *Classics in Applied Mathematics*. Society for Industrial and Applied Mathematics (SIAM), Philadelphia, PA, 2011.
- [28] T. Kato. *Perturbation theory for linear operators*. Classics in Mathematics. Springer-Verlag, Berlin, 1995. Reprint of the 1980 edition.
- [29] J. Meng, Y. Zhang, and L. Mei. A virtual element method for the Laplacian eigenvalue problem in mixed form. *Appl. Numer. Math.*, 156:1–13, 2020.
- [30] D. Mora and G. Rivera. *A priori* and *a posteriori* error estimates for a virtual element spectral analysis for the elasticity equations. *IMA J. Numer. Anal.*, 40(1):322–357, 2020.
- [31] D. Mora, G. Rivera, and R. Rodríguez. A virtual element method for the Steklov eigenvalue problem. *Math. Models Methods Appl. Sci.*, 25(8):1421–1445, 2015.
- [32] D. Mora, G. Rivera, and I. Velásquez. A virtual element method for the vibration problem of Kirchhoff plates. *ESAIM Math. Model. Numer. Anal.*, 52(4):1437–1456, 2018.
- [33] D. Mora and I. Velásquez. A virtual element method for the transmission eigenvalue problem. *Math. Models Methods Appl. Sci.*, 28(14):2803–2831, 2018.
- [34] D. Mora and I. Velásquez. Virtual element for the buckling problem of Kirchhoff-Love plates. *Comput. Methods Appl. Mech. Engrg.*, 360:112687, 22, 2020.
- [35] P.-A. Raviart and J.-M. Thomas. *Introduction à l'analyse numérique des équations aux dérivées partielles*. Collection Mathématiques Appliquées pour la Maîtrise. [Collection of Applied Mathematics for the Master's Degree]. Masson, Paris, 1983.
- [36] O. Čertík, F. Gardini, G. Manzini, L. Mascotto, and G. Vacca. The  $p$ - and  $hp$ -versions of the virtual element method for elliptic eigenvalue problems. *Comput. Math. Appl.*, 79(7):2035–2056, 2020.

KING ABDULLAH UNIVERSITY OF SCIENCE AND TECHNOLOGY (KAUST), SAUDI ARABIA

*Email address:* `daniele.boffi@kaust.edu.sa`

*URL:* `http://cemse.kaust.edu.sa/people/person/daniele-boffi`

DIPARTIMENTO DI MATEMATICA "F. CASORATI", UNIVERSITÀ DI PAVIA

*Email address:* `francesca.gardini@unipv.it`

*URL:* `http://www-dimat.unipv.it/gardini/`

DICATAM, UNIVERSITÀ DI BRESCIA, ITALY

*Email address:* `luca.gastaldi@unibs.it`

*URL:* `http://luca-gastaldi.unibs.it`